

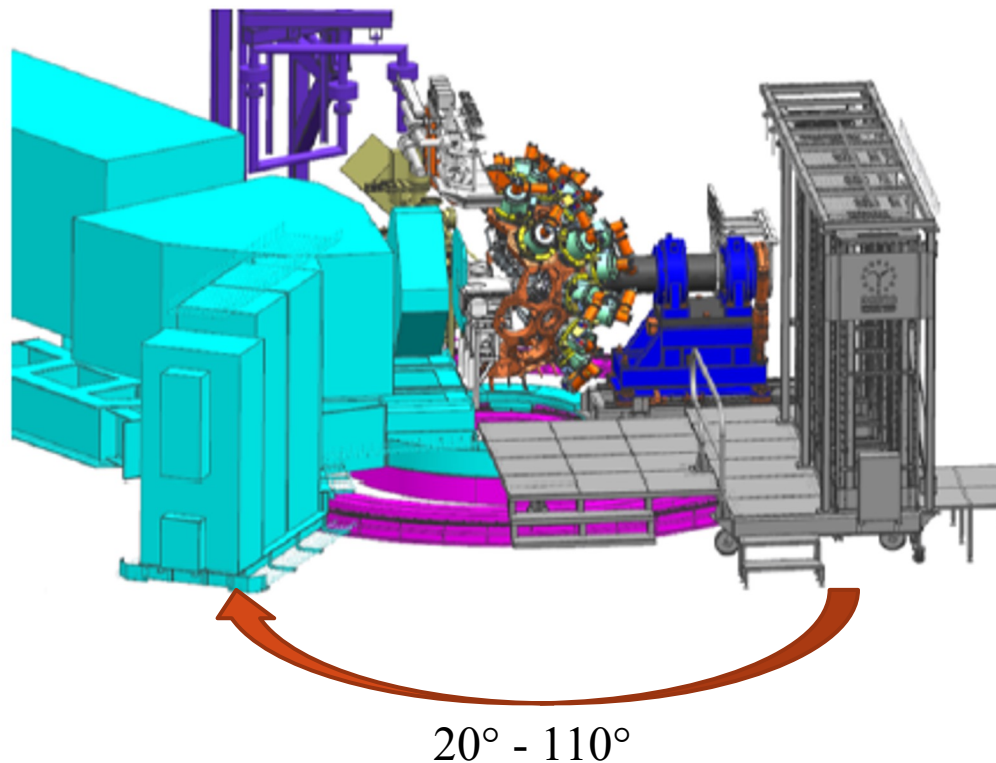
Detectors for Gamma Radiation

Francesco Sgarbossa

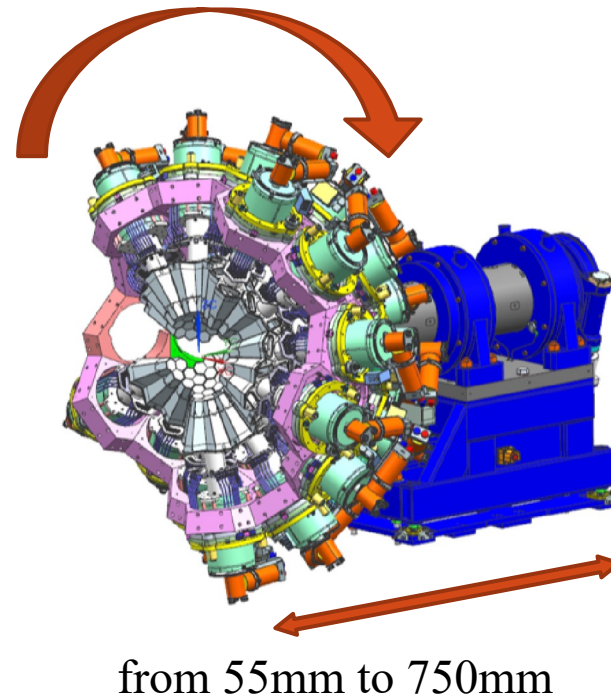
INFN-LNL and University of Padova

Advance GAMMA Tracking Array installation at LNL-INFN

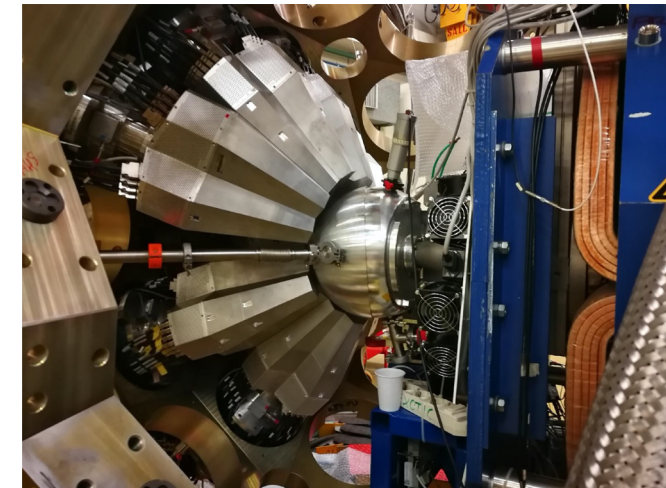
AGATA at LNL in a 2π configuration is the phase 2 of AGATA. At LNL-INFN AGATA couple with PRISMA will consist of up to 27 AGATA triple clusters (ATCs) out of the 30 possible due to the mechanical constrain to get the beam line through.



$\pm 85^\circ$ along its axis



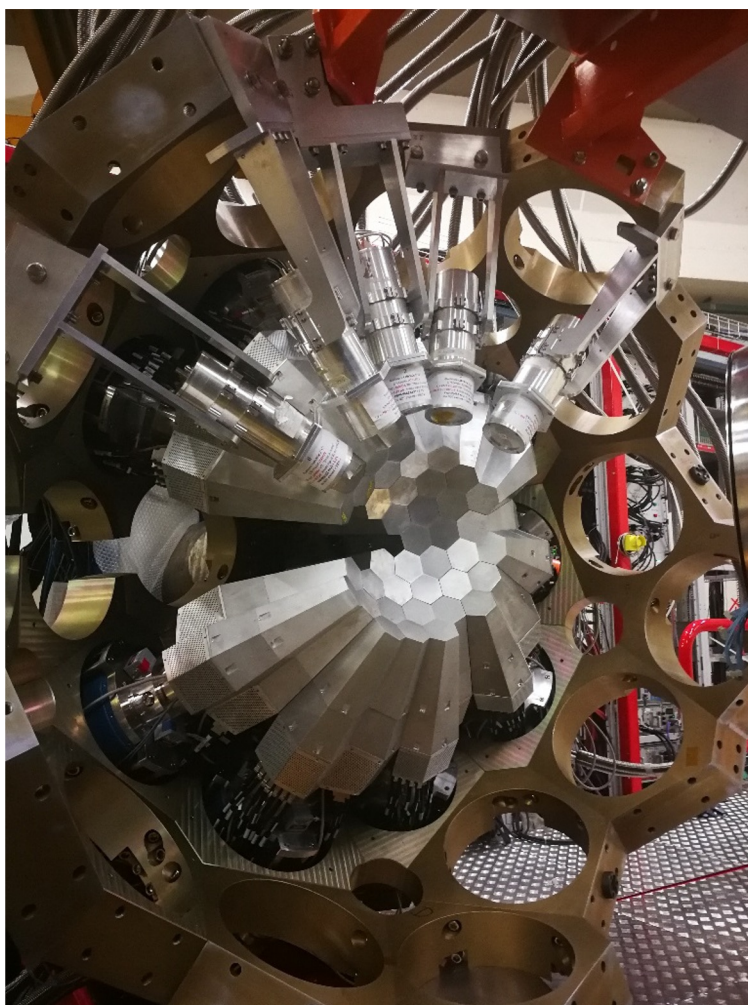
13 ATCs installed close to the reaction chamber



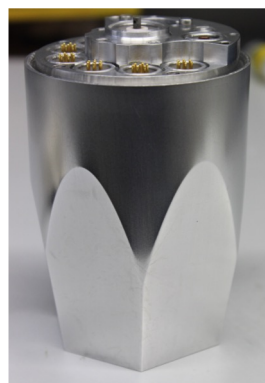
AGATA at LNL-INFN

13 ATCs installed (27 HPGe detector)

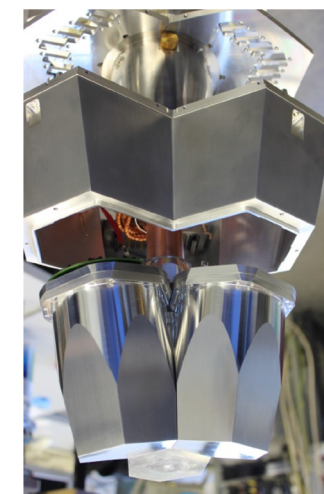
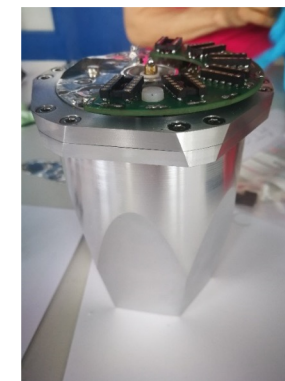
n-HPGe encapsulated detector with 36 segments + 1 core



OLD encapsulated HPGe detector
standard annealing (few days at
 102°C), roughly one out of three
annealed capsules would suffer from
leakage current

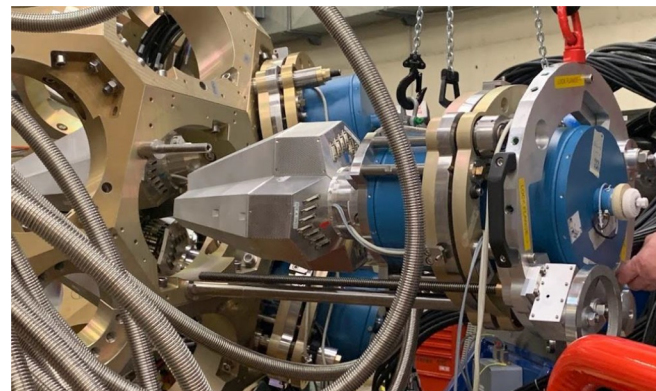
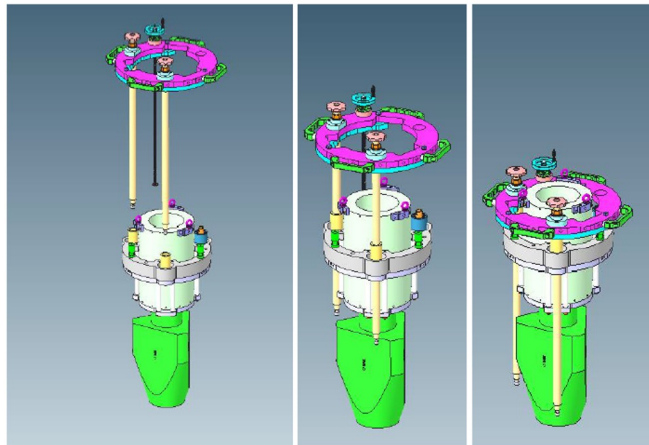


NEW encapsulated HPGe detector
new annealing method by MIRION:
capsules connected to a pumping
system during annealing

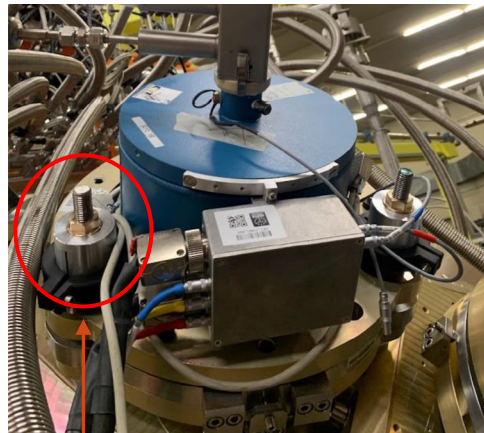


AGATA array installation at LNL-INFN

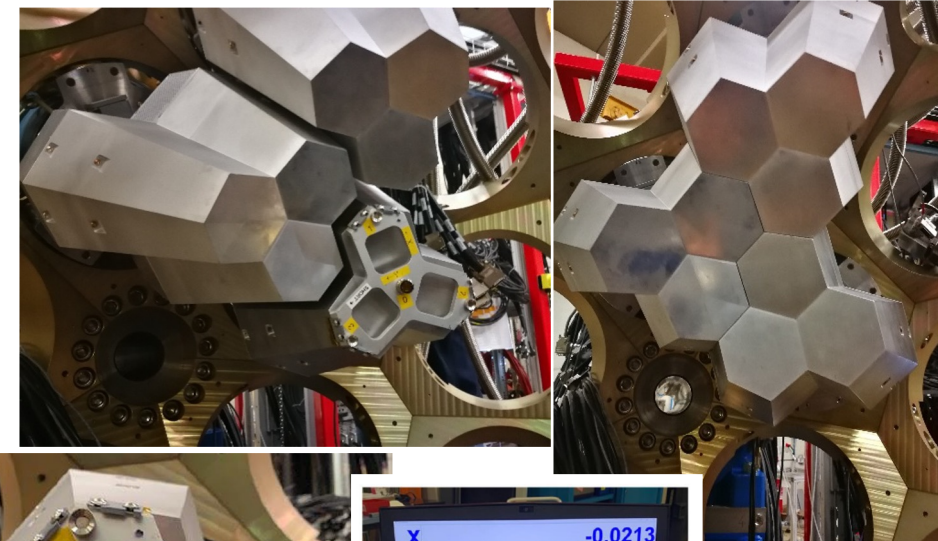
Handling Fixture: mounting the ATC in horizontal way



Mechanics upgrade: precise control on the ATC placement



Laser alignment: New laser tool (x,y,z) to align ATC on the AGATA array



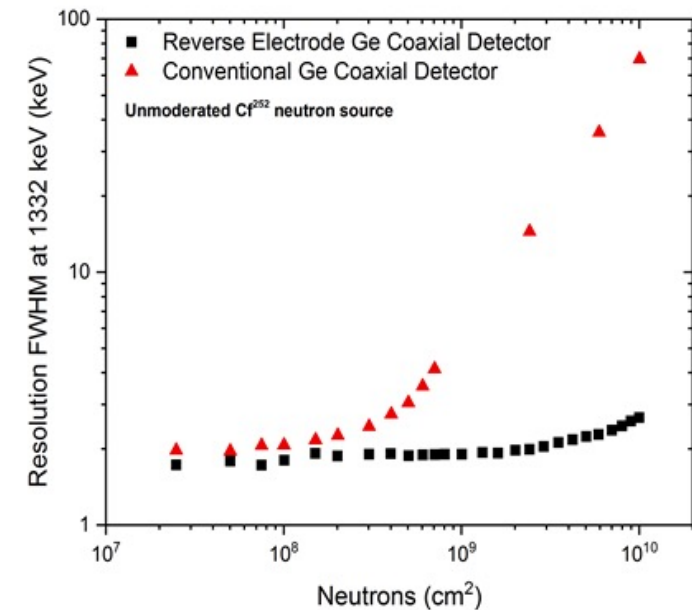
HPGe segmented detector research limits

Limitation on segmented position sensitive n-HPGe detectors: **Li n contacts** forms > 0.5 mm junction.

- dead layer where no charge collection occurs ¹
- not stable under annealing treatments for damage recovery ²
- prevents stable and thin segmentation

Segmentations are currently performed on the p⁺ boron side.

- holes are much more subjected to trapping induced by neutron damage -> worse resolution ³



Resolution detrimental effects after neutron radiation exposure in hall (red) and electron (black) collecting non segmented HPGe [4]

1) J. Eberth et al. *Particle and Nuclear Physics* **60** 283 (2008)

2) P. N. Peplowski et al *NIMA* **942** (2019)

3) H. W. Kraner et al. *IEEE Transactions on Nuclear Science* **27**, 1 (1980)

4) R. H. Pehl et al. *IEEE Transactions on Nuclear Science*, **26**, 1 (1979)

N3G: Next Generation Germanium Gamma Ray Detectors

- Fabrication of p-HPGe detector using a new doping technique: **pulsed laser melting** ¹.
200-300 nm junction for n and p side without bulk contamination ².
- New generation of electronics, DAQ and cryostat for this technology
- Performance and rad-hardness test



CALL CSNV

1. Planar detector prototype (PRONG- INFN)
2. Coaxial geometry upgrade

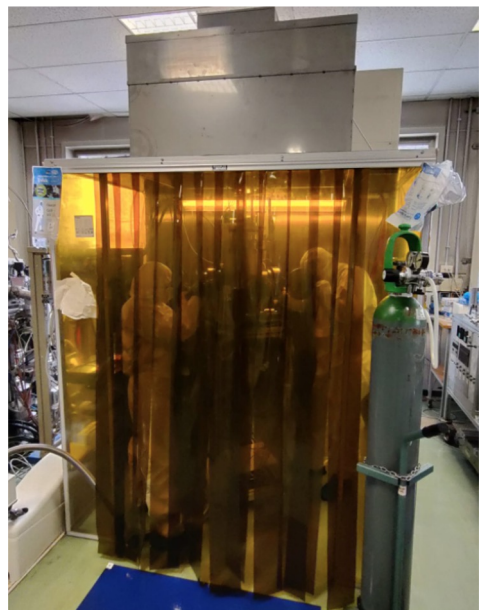
1. n-side segmentation
2. Higher active volume
3. Easy segmentation: 300nm junctions
4. Lower annealing deterioration

RETURN TO

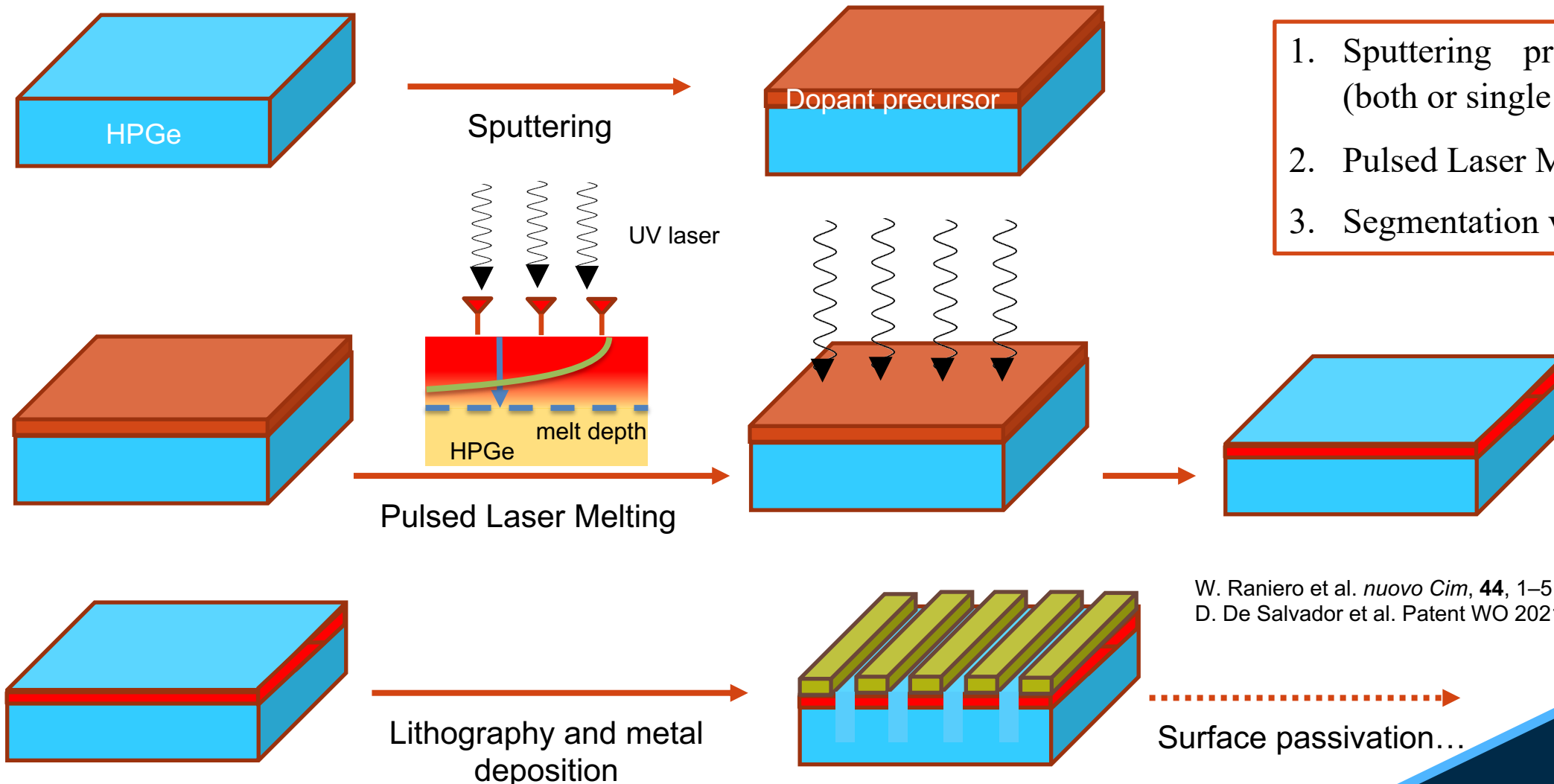
1. International gamma ray community
2. INFN CSN3: new detector
3. Detector repair infrastructure @ LNL

1) G. Maggioni et al. *Eur. Phys. J. A*, **54**, 34 (2018)

2) V. Boldrini et al. *J. Phys. D. Appl. Phys.*, **52**, 11 (2019)



N3G approach: from planar to coaxial detector



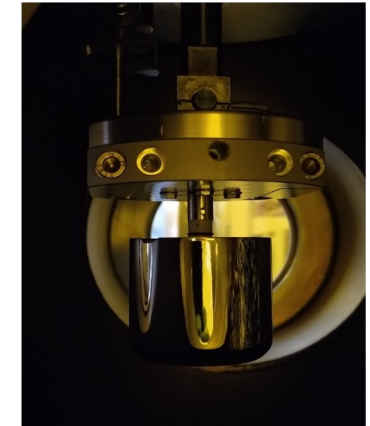
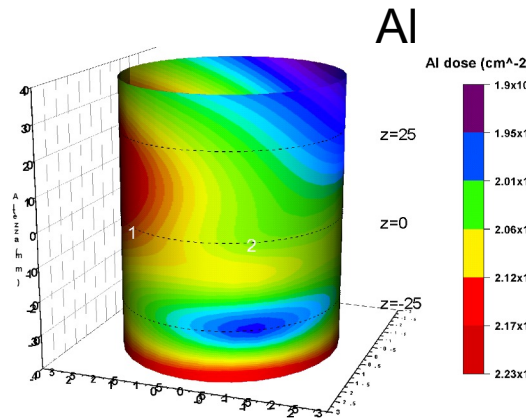
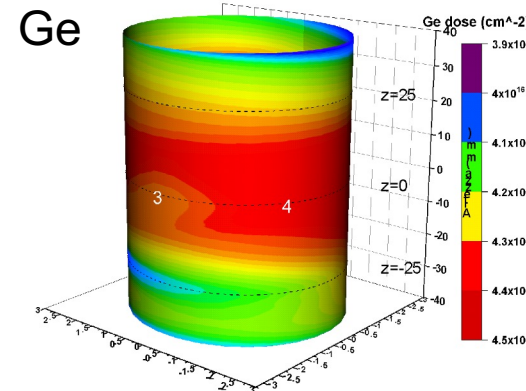
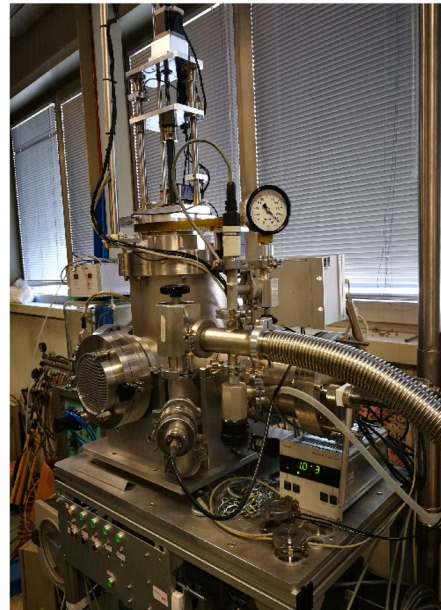
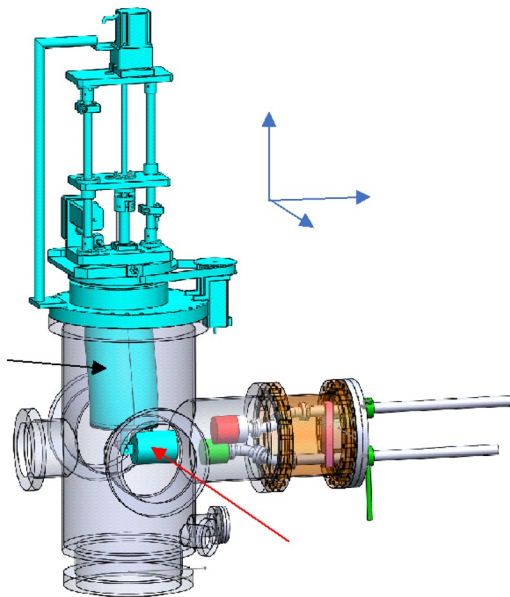
1. Sputtering precursor deposition (both or single n, p side)
2. Pulsed Laser Melting diffusion
3. Segmentation via lithography

W. Raniero et al. *nuovo Cim*, **44**, 1–5 (2021)
 D. De Salvador et al. Patent WO 2021/214028 A1

Fabrication – Dopant deposition

Dopant precursor deposited by sputtering process

- Coaxial sputtering geometry machine development
- 3D dopant homogeneity

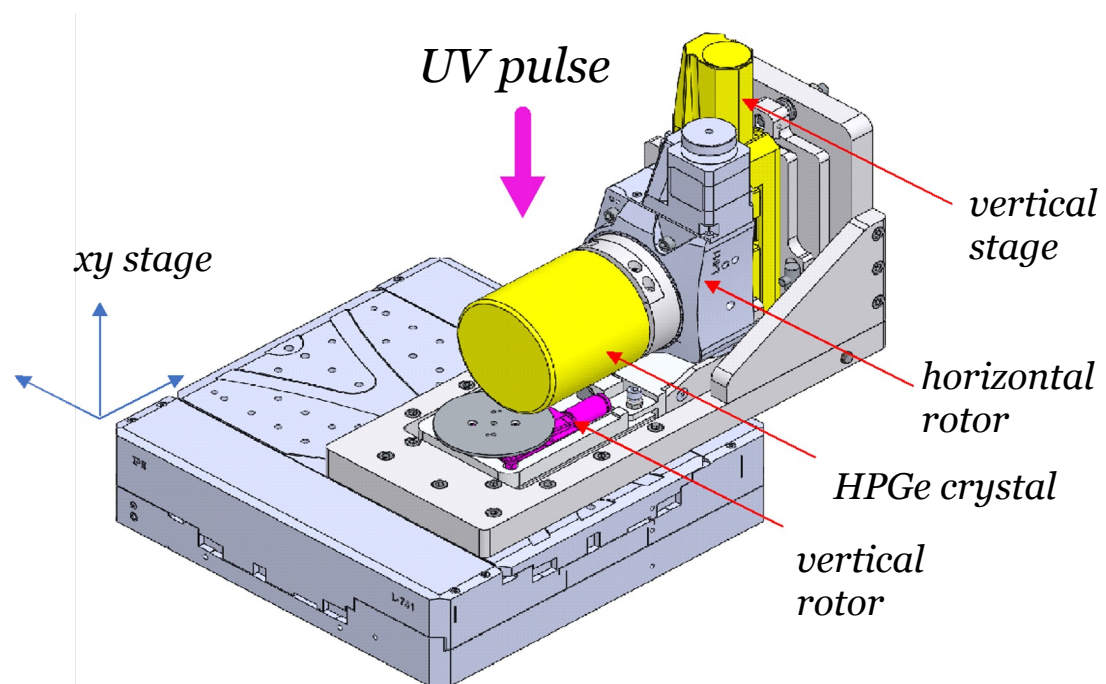


Homogeneity precursor reconstruction using RBS analysis

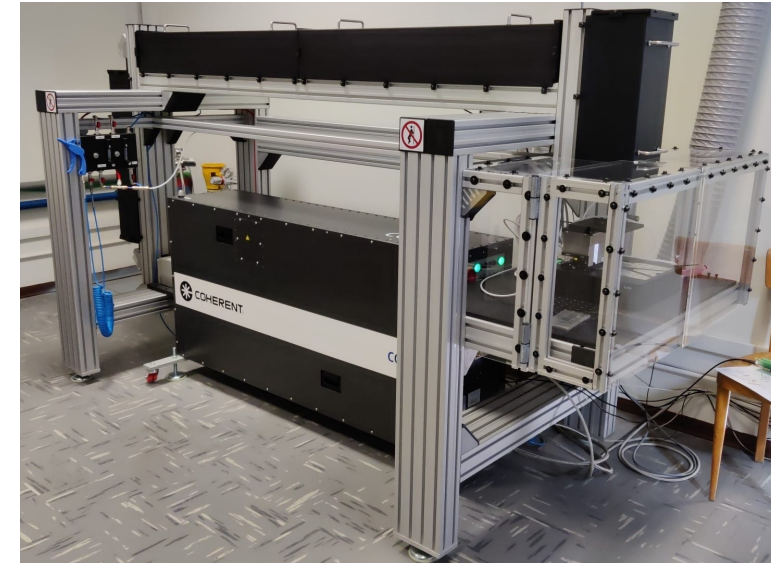
Fabrication – dopant diffusion & junction formation

Dopant diffusion by pulsed laser melting

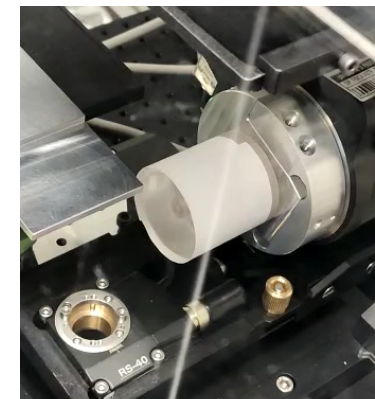
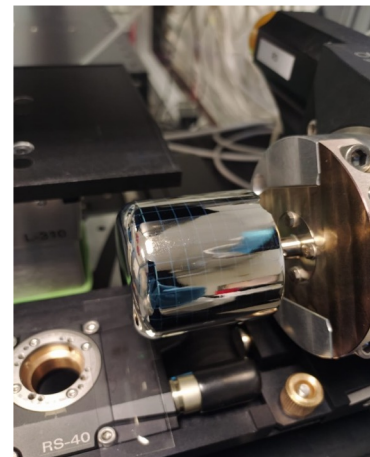
- Huge previous studies (and a patent) on diffusion via PLM
- Coaxial handling system for surfaces exposure to UV laser pulses



Scheme of the laser sample holder



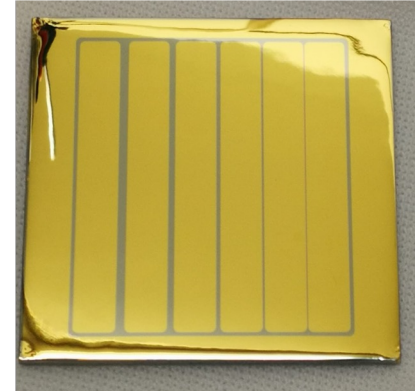
PLM system @ UNIPD



Fabrication – lithography for segmentation

Lithography systems

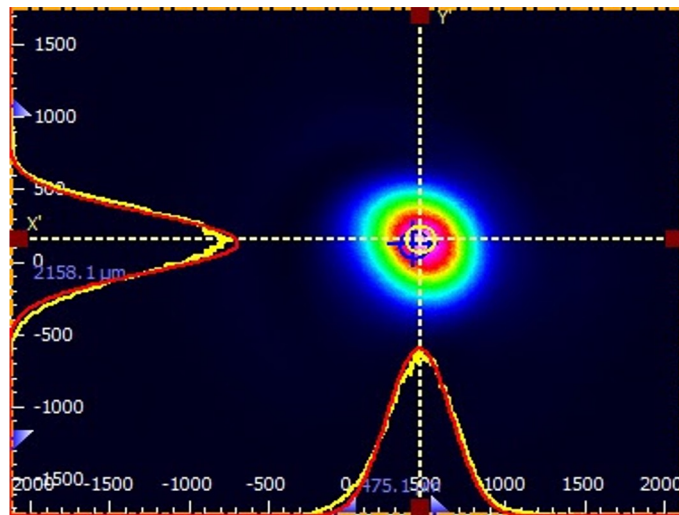
- Studies using planar HPGe geometry
- Robotic 3D lithography system for coaxial detector segmentation.



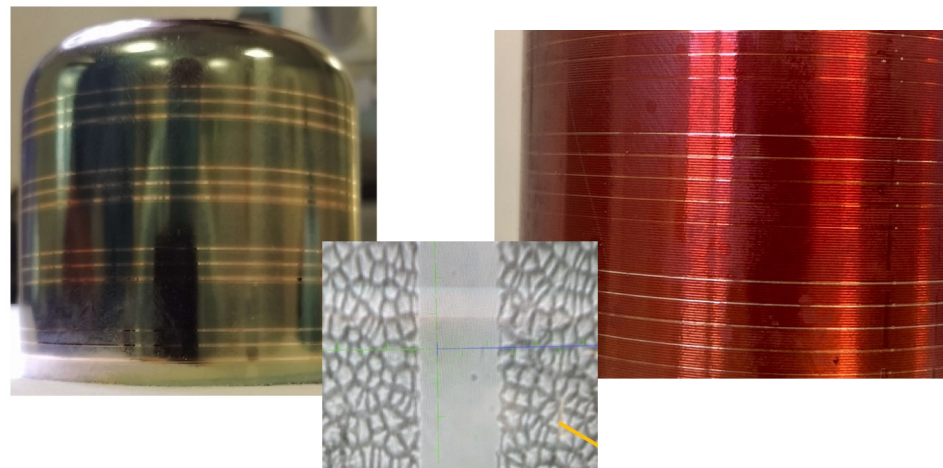
segmented planar detector – variable trench



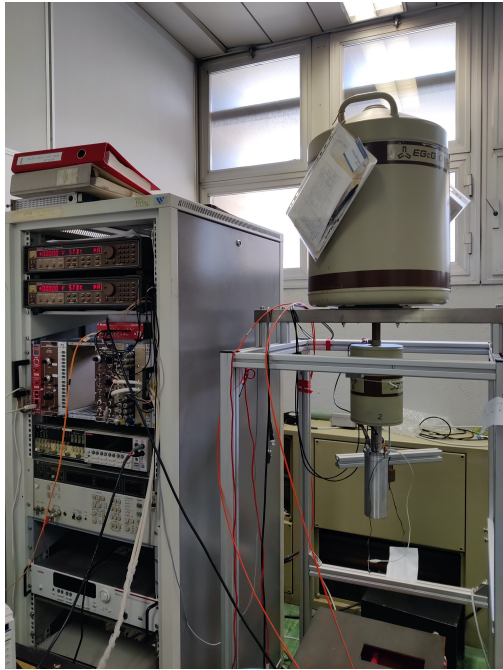
3D lithography system



Laser for lithography : lateral beam profile



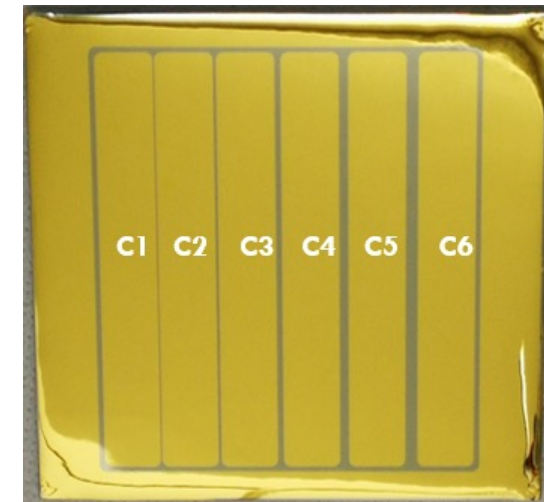
Lithographic tests on coaxial dummy



Detector test: planar results

PLANAR segmented n side Sb PLM / p side with Al PLM

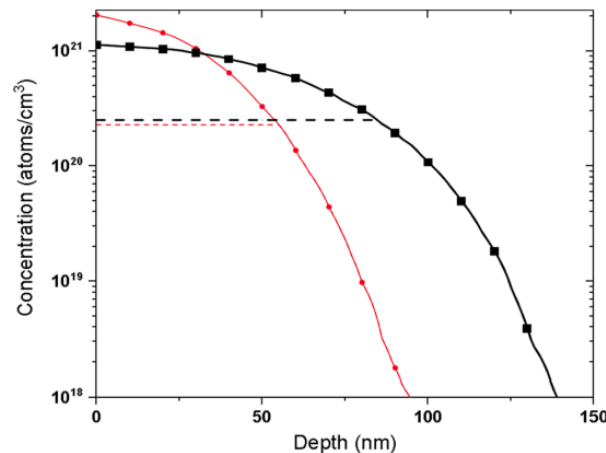
^{133}Ba normalized spectra; before annealing (black data) and after annealing (red data). P+ Al side (without guard ring) and C1 segment Sb (with guard ring). Annealing = 100°C 40h. -15 V polarization.



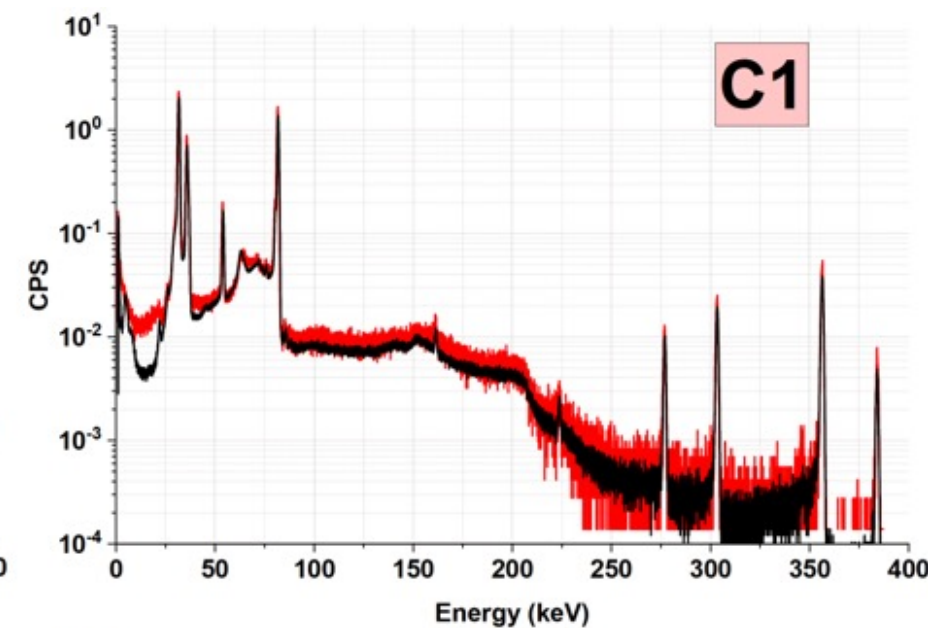
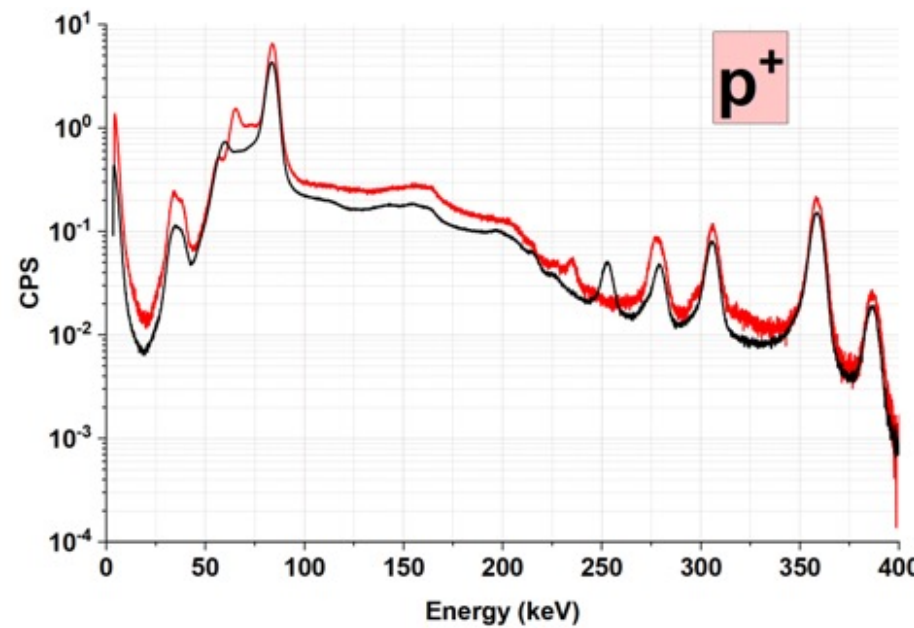
S. Bertoldo et al. *Eur. Phys. J. A*, **57**, 1–10 (2021)

segmented planar detector – Sb n contact

Lab for coaxial detector test @ LNL



SIMS Sb profile, with electrical activation



Monolayer doping: the future for detector junction?

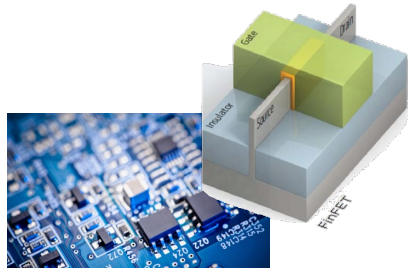


UNIVERSITÀ
DEGLI STUDI
DI PADOVA

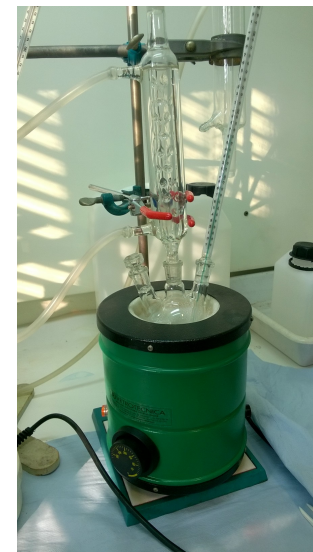
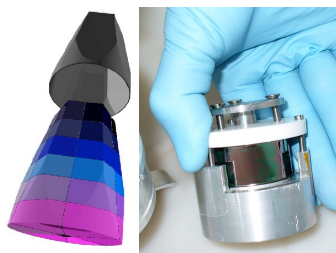
Use of molecular precursor reacting with Ge surface to form a self-limited monolayer ^{1,2}

- Extremely controlled amount of dopant
- Coaxial 3D geometry compatible: conformal deposition
- Adsorption process at different temperature
- Compatible with PLM ^{2,3}

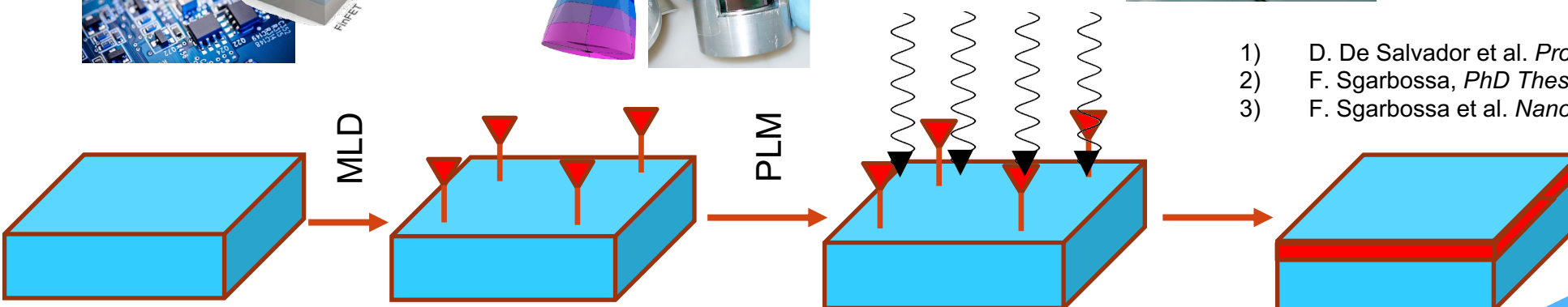
Nanoelectronics



γ-Ray detectors



MLD deposition process @ UNIPD and LNL



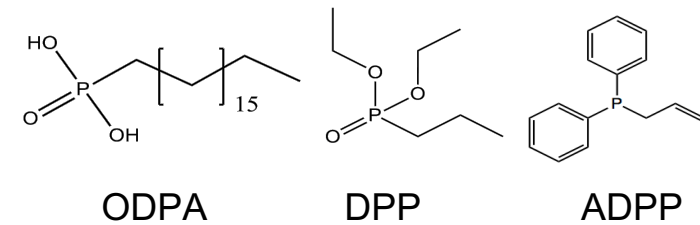
- 1) D. De Salvador et al. *Proceedings*, **26**, 1, 39 (2019)
- 2) F. Sgarbossa, *PhD Thesis*, Univ. of Padova (2019)
- 3) F. Sgarbossa et al. *Nanotechnology*, **29**, 465702 (2018)



Monolayer doping: n type dopant studies

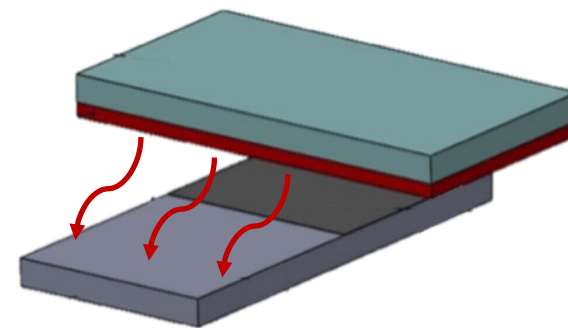
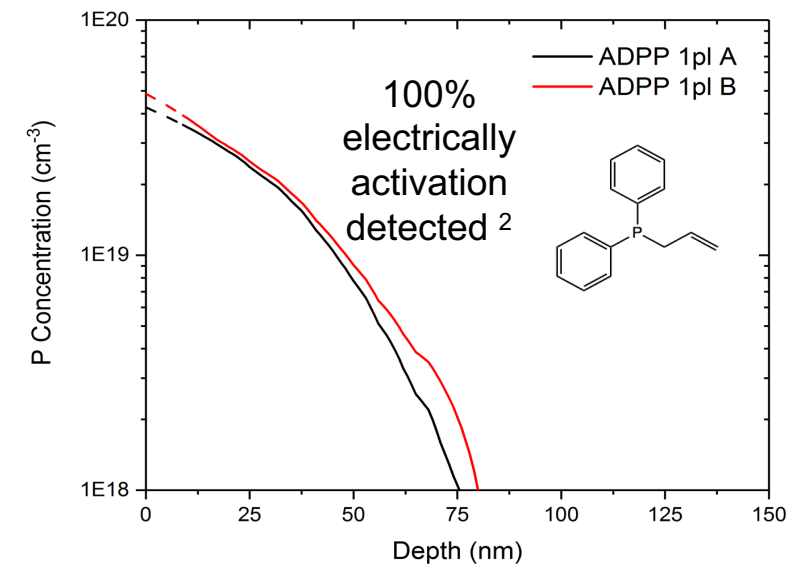
Three different phosphorus molecular precursor studied ^{1,2}

- ADPP found as the best precursor: electrically active after PLM ²
- PLM treatment guarantee no bulk contamination



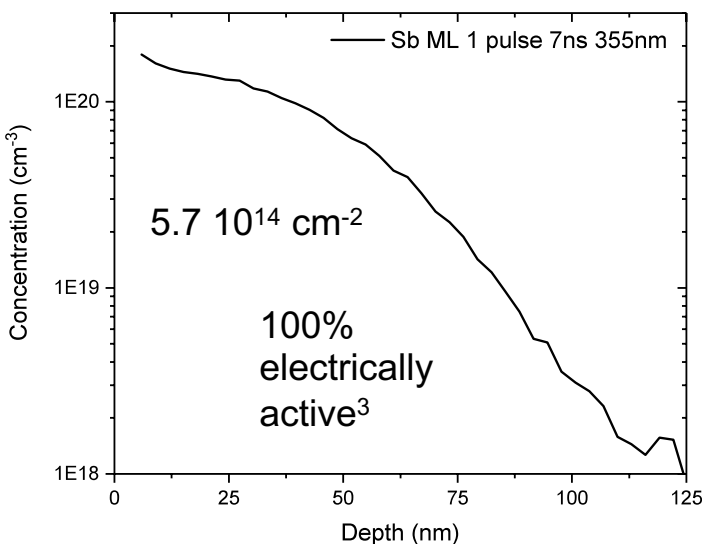
Antimony monolayer formation studied: diffusion via PLM tested ³

- Sb ML deposition at high temperature could be an issue for contamination

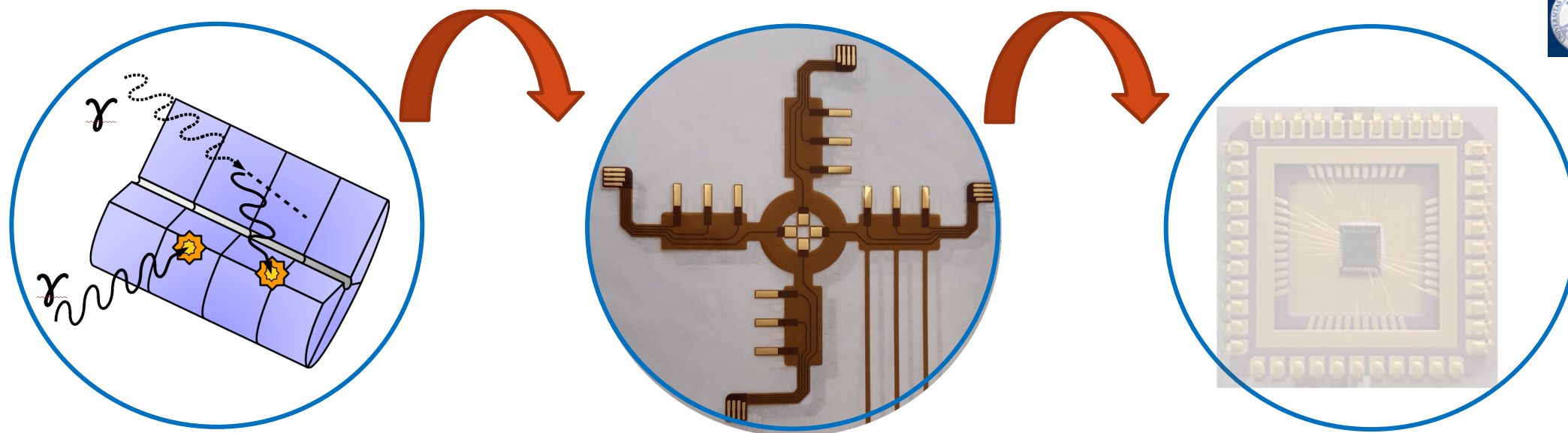


Sb gas monolayer adsorption geometry ³

- 1) F. Sgarbossa et al. *Nanotechnology*, **29**, 465702 (2018)
- 2) F. Sgarbossa et al. *Appl. Surf. Sci.* **541**, 148532 (2021)
- 3) F. Sgarbossa et al. *Appl. Surf. Sci.* **496**, 143713 (2019)



Front End Electronics for HPGe coaxial & segmented detectors



- The external electrodes of the detector are connected to the Charge Sensitive Preamplifier (CSP) through a **flexible PCB** to be wrapped around the detector itself
- The connection system is designed so that **it doesn't scratch and damage** the surface of the electrodes
- With respect to the state-of-the-art HPGe read-out chain, the Charge Sensitive Pre-amplifiers is realized in integrated technology. In such a way it is:

MORE COMPACT

MORE EFFICIENT

LESS POWER CONSUMING



Nuclear Physics
Mid Term Plan in Italy



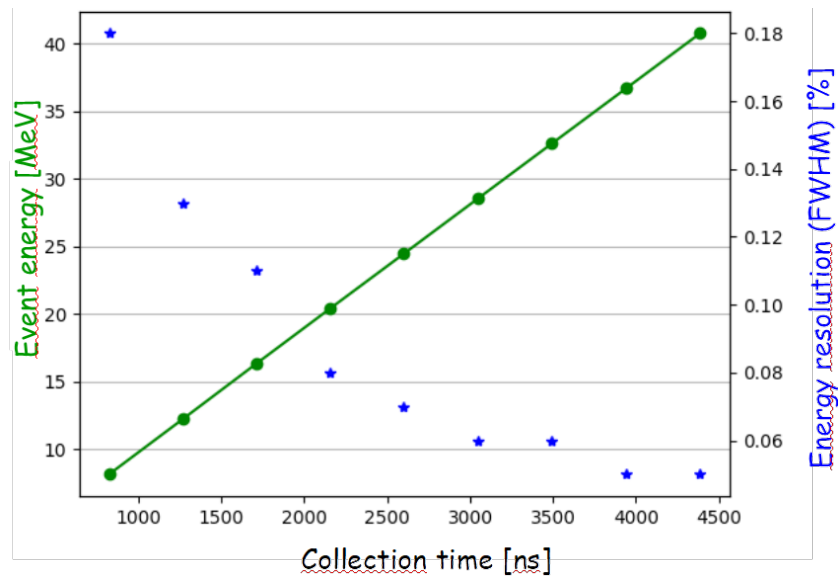
The ASIC (Applied Specific Integrated Circuits)

- It is characterized by **6 mW power consumption** and **8 MeV dynamic range**, which can be extended up to **40 MeV** thanks to an innovative

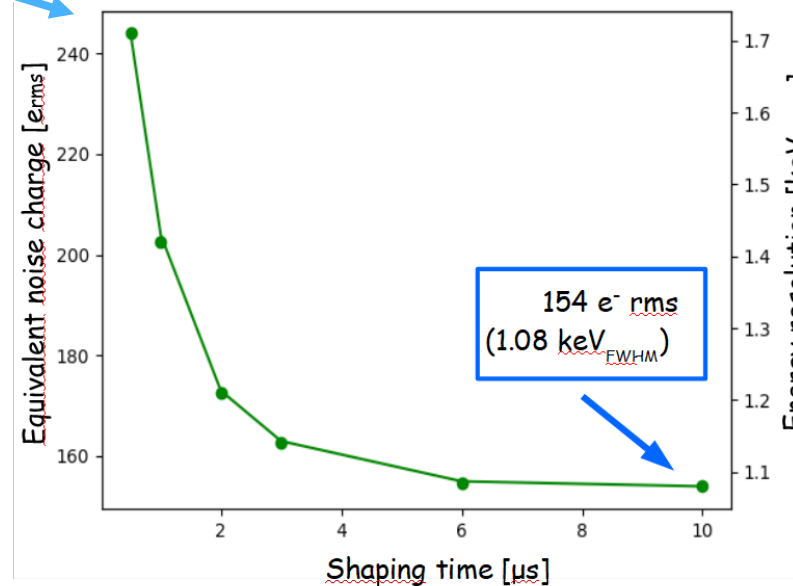
FAST RESET CIRCUITS →

- It is a

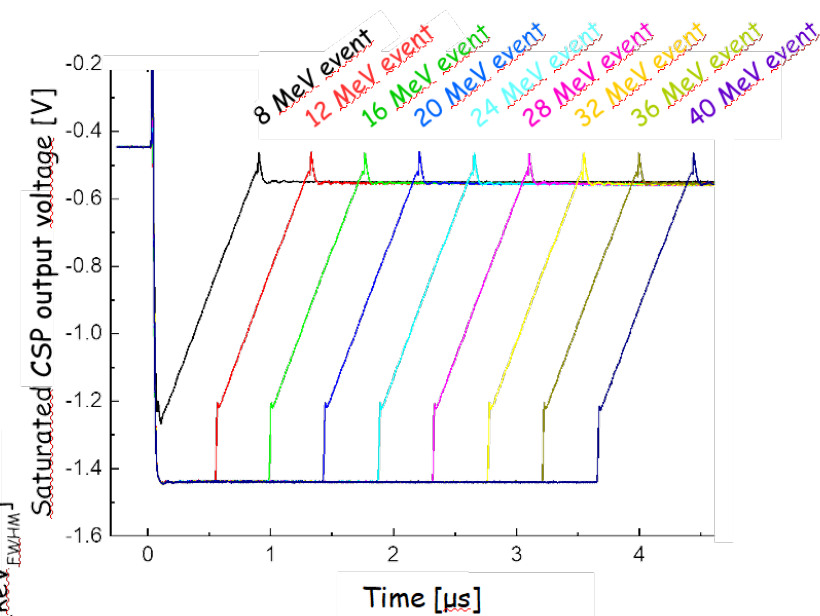
LOW NOISE DEVICE →



Linearity and energy resolution in fast-reset mode: for events with energy greater than 15 MeV the resolution, expressed as FWHM, is better than 0.11 %



Resolution measurements on 1 MeV simulated events and 15 pF detector capacitance

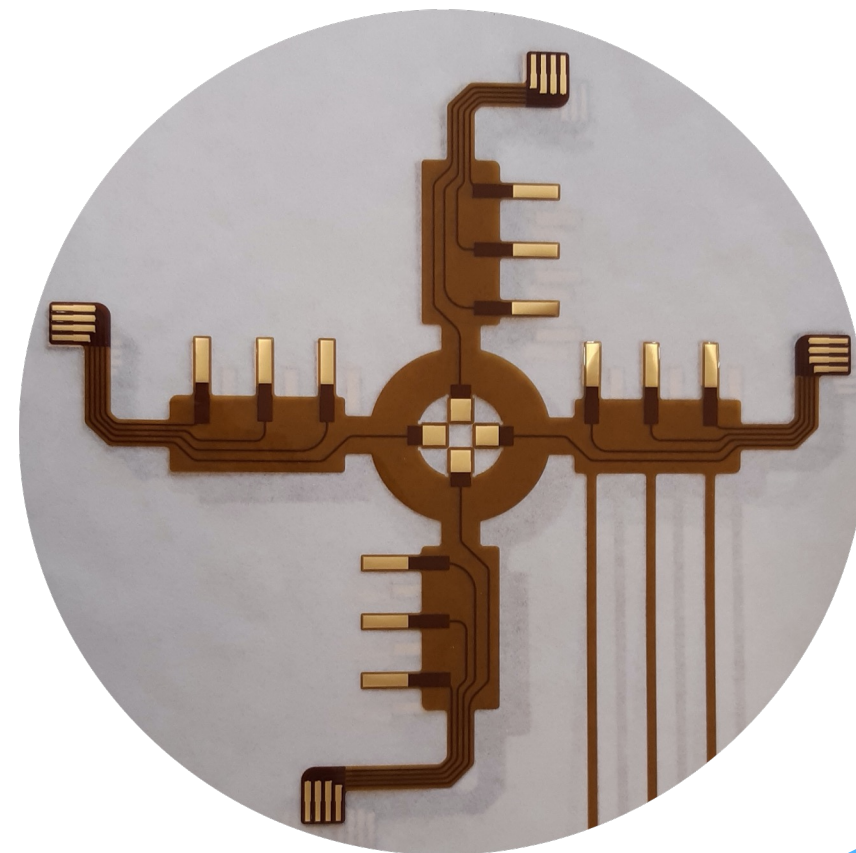


CSP in saturation: the time-duration of this condition is proportional to the incident energy

S. Capra et al. *IEEE Transactions on Nuclear Science*, 69, 7, 1757-1764 (2022)

Challenges

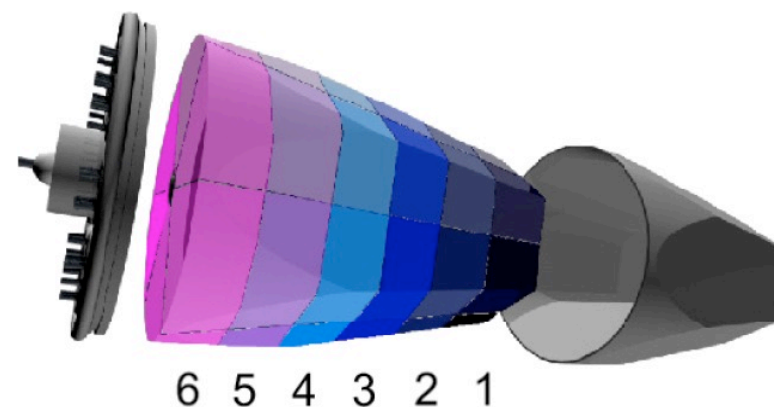
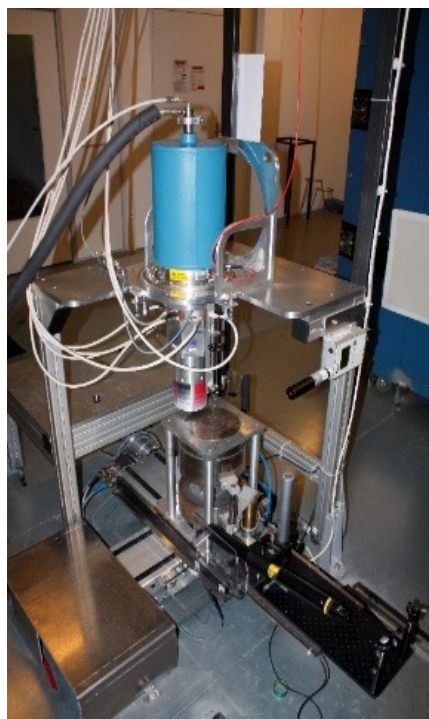
- **Resolution improvements.**
- Direct application in **cryogenic environments.**
 - **Thermal noise reduction.**
 - **No parasitic capacitances** introduced by long cables and connections.
 - Particularly **challenging** because at the state-of-the-art there is no model describing the transistors working behaviors at cryogenic temperature (liquid-nitrogen or liquid argon) to be used in simulations.



Agata capsule scan: LNL-IPHC collaboration

AGATA DETECTOR

- Encapsulated coaxial N-type detector
- 6x6 segments \rightarrow 37 chan. per crystals



IPHC SCANNING TABLE

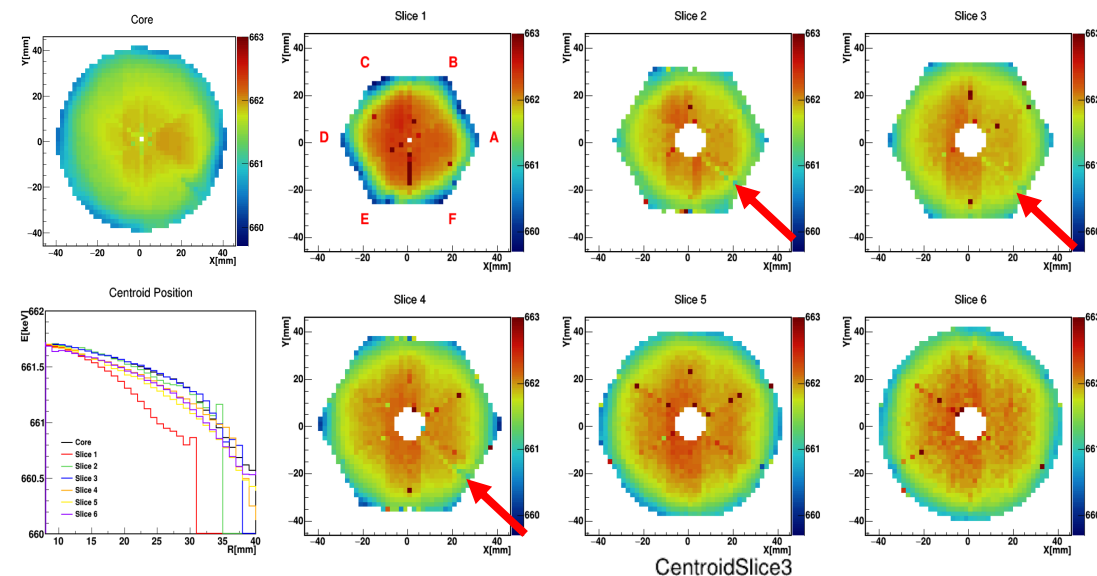
- Encapsulated coaxial N-type detector
- Intense source in a collimator (diam 1 mm, 165 mm) X Y mov. by mm or μm steps
- 14-bit, 100 MHz home made digital electronics (TNT2)
- Labview GUI alternating collimator move, data acquisition and liquid N2 fills

F.C.L. Crespi et al., NIM A 593(3), 440–447 (2008)

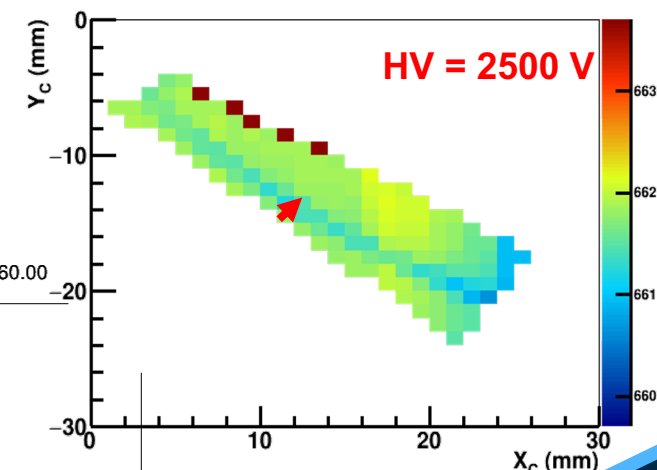
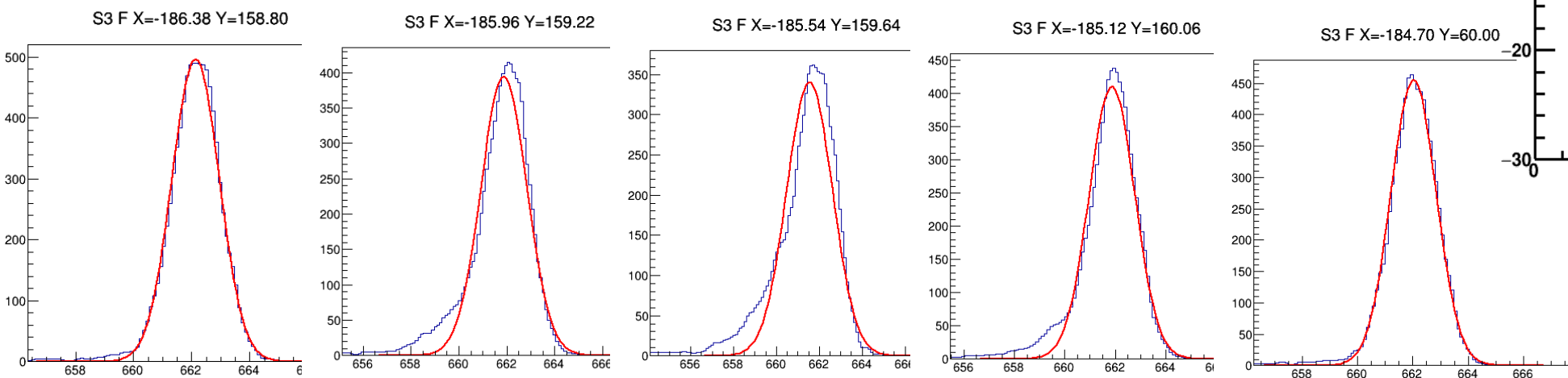
Electron trapping studies

ENERGY PEAK SHIFT

- Detector scanned in vertical position
- ^{137}Cs source (662 keV) used for scanning
- Gamma-ray spectrum collected at each XY position
- Peak shift plotted vs XY/segment slice
- Anomaly observed in slices 2, 3 and 4 (red arrows)



100 μm pitch along the diagonal with 1 mm diam
collimator $R \sim 15.6$ mm



Electron trapping studies

A lot of scans for detailed study of the trapping anomaly but also of the normal electron trapping.

- Geometry of the anomaly - transverse scans
- Trapping half-life - scans using different amplifier shaping time constants
- Collection efficiency - scans vs HV
- Trap depth - scans vs crystal temperature



LNL-IPHC COLLABORATION AND PROSPECTIVES

- Scans of passivated surfaces
- Scans of laser implanted contacts with or without segmentation (N3G)
- Scans of any contact/passivated surfaces with or without coating
- Surface/volume exploration with low/high gamma-ray energies (^{241}Am 60 keV, ^{137}Cs 662 keV, ^{152}Eu from 122 to 1408 keV)

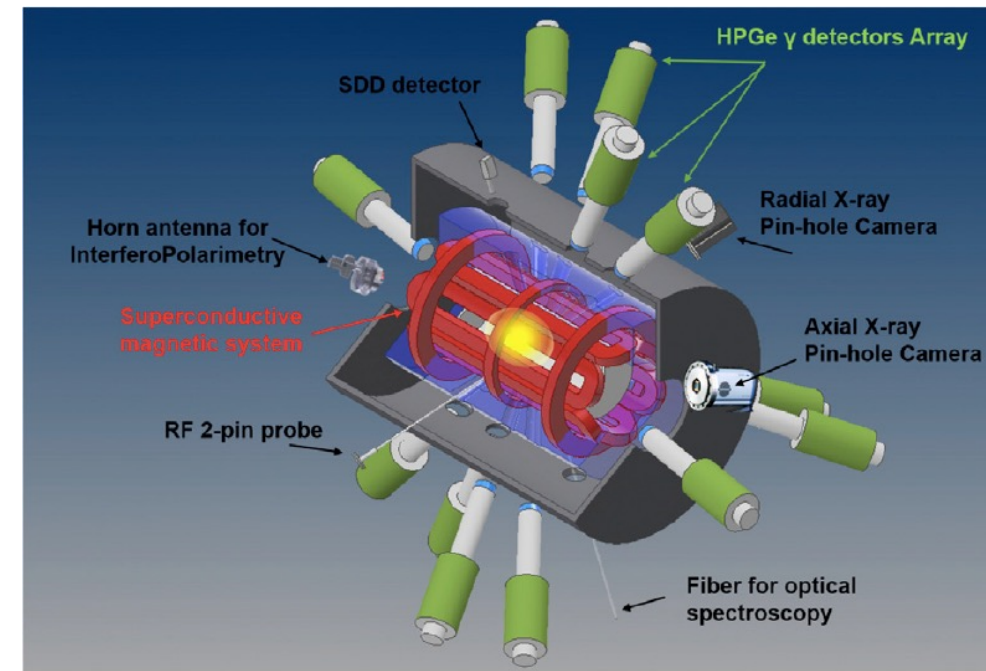
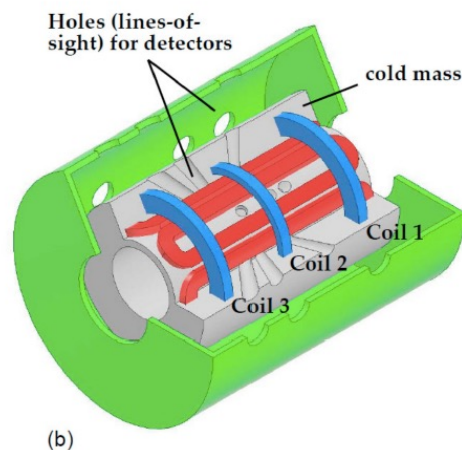
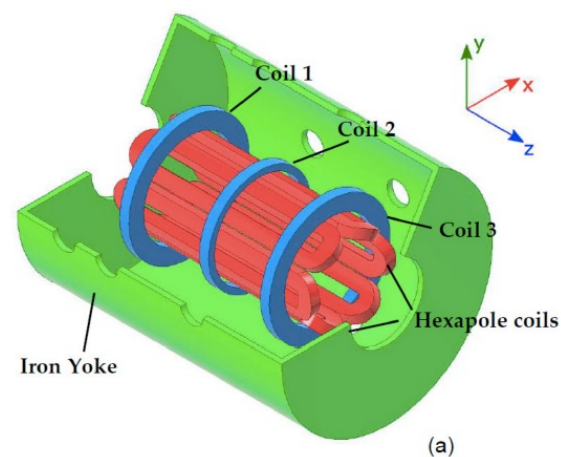


PANDORA (Plasma for Astrophysics, Nuclear Decay Observation and Radiation for Archeometry)

Measure, for the first time in plasma, nuclear beta-decay rates of radionuclides involved in nuclear-astrophysics processes.

Compact magnetic plasma trap has been designed to reach the needed plasma densities, temperatures, and charge-states distributions to emulate stellar-like conditions.

The decay rate of the radionuclides will be measured through the detection of the γ -rays emitted by the excited daughter nuclei following the β -decay.

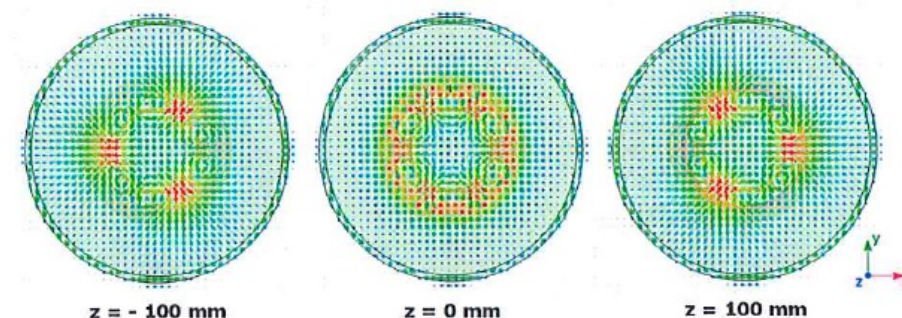
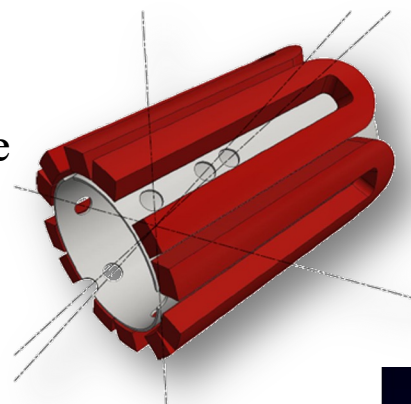


Required Ge array

An array of 14 HPGe detectors placed around the trap will be required to detect the emitted γ -rays.

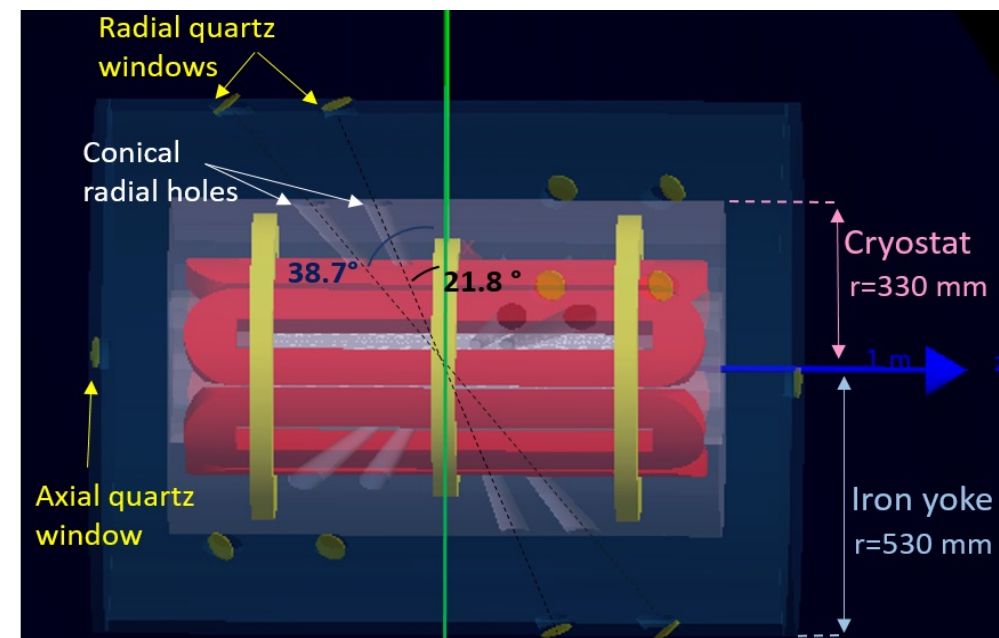
Main limitations arises from:

- **Size of coils of the magnetic trap**
- **Magnetic branches:** region of the magnetic trap where the B field lines are more intense – high bremsstrahlung induced gamma and x-rays.



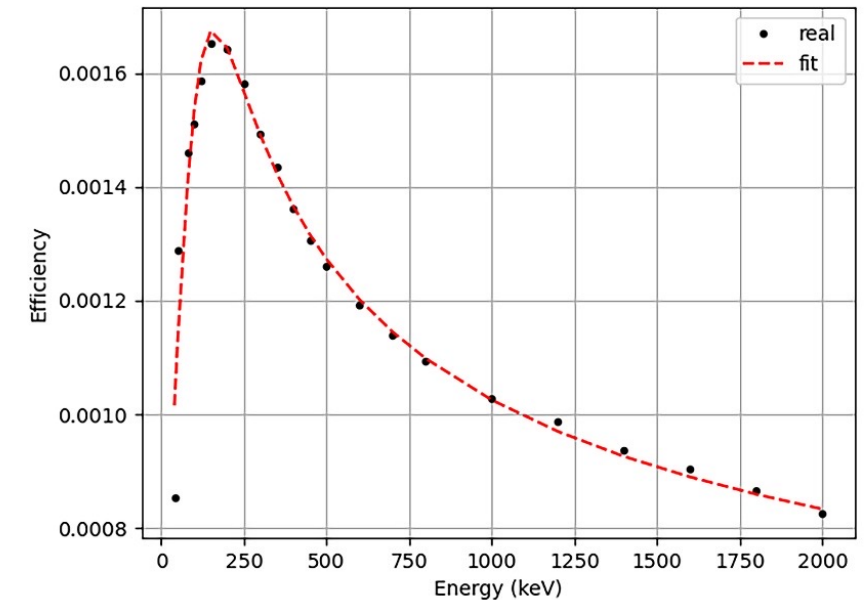
The cryostat structure: holes are created along the conductor hexapole interspaces in order to use it as multi-collimator and suppress the background coming from the magnetic trap.

Iron yoke surrounding the magnetic plasma trap is shown in blue. Quartz windows (in yellow) are placed in correspondence with conical holes.



HPGe array for PANDORA

- Photopeak detection efficiency (interplay between detector number and mechanical constraint)
- Signal to noise ratio (high background self-generated inside the trap)
- ➔ Harsh experimental conditions (sufficiently fast response from detectors: counting rate of 50kHz on each detector)
- Magnetic field effects on HPGe charge collection ($B < 200$ gauss)

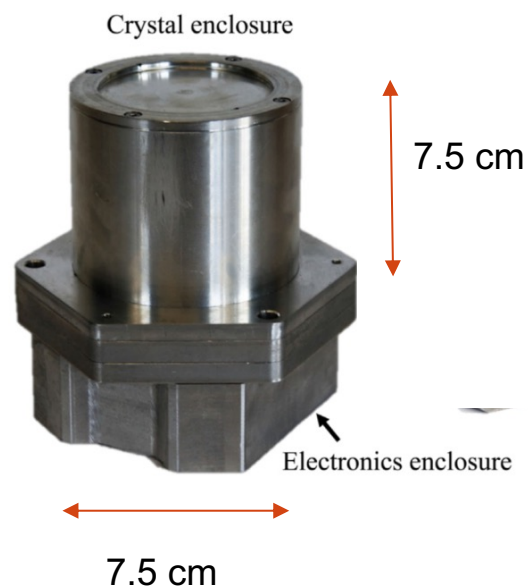


Photopeak detection efficiency vs. gamma-ray Energy

Normal Working conditions will require:

- LN₂ Cooling system for HPGe array is under study
- A new lab to store, repair and perform the maintenance of detectors

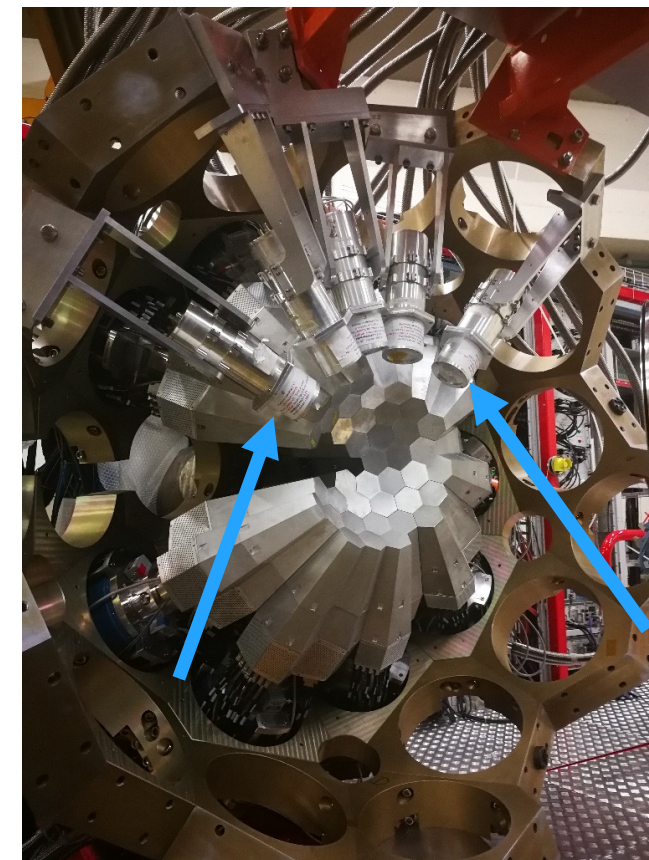
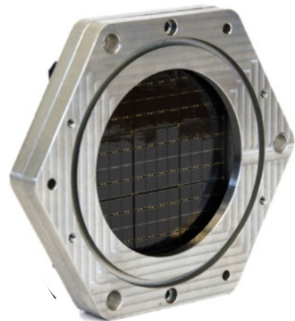
LaBr₃:Ce:Sr + SiPMs



General features:

- The crystal is a LaBr₃:Ce:Sr cylinder 7.5 cm high with a diameter of 7.5 cm.
- The detector uses 144 SiPMs and 9 ASICS,
- Each SiPM has 40000 30x30 micron SPADs
- The detector uses a variable gain selected on an event by event basis
- The detector has also an USB based digital embedded DAQ (C++ based)
- The maximum count rate at which the resolution is not degraded is 40kHz

SiPM MATRIX



AGATA array at LNL with 5 LaBr₃ installed (read from PMT, not SiPMs yet).

F.Camera^{1,3}, O.Wieland³, A.Bracco^{1,3}, F.C.L. Crespi^{1,3}, S.Leoni^{1,3}, B.Million³,
C.Fiorini^{2,3}, M.Agnolin^{2,3}, G.Borghini^{2,3}, M.Carminati^{2,3}, D.Di Vita^{2,3}, G.Ticchi^{2,3}

¹ Università di Milano, Dipartimento di Fisica, via Celoria 16, 20133 Milano, Italia

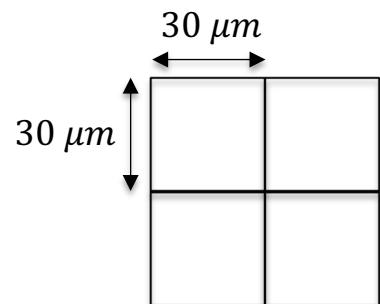
² Politecnico di Milano, Dipartimento di Elettronica, Informazione e Bioingegneria, piazza L. da Vinci 32, 20133 Milano, Italia

³ INFN sez. Milano, via Celoria 16, 20133 Milano, Italia

FBK NUV-HD SiPMs custom tile

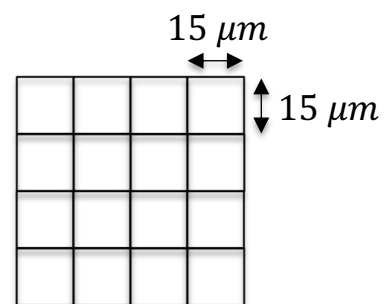
- 1" x 1" size, 4-side buttable
- Custom high-reliability connectors
- Temperature sensor under each tile

Two cell options: 30 μ m and 15 μ m cells



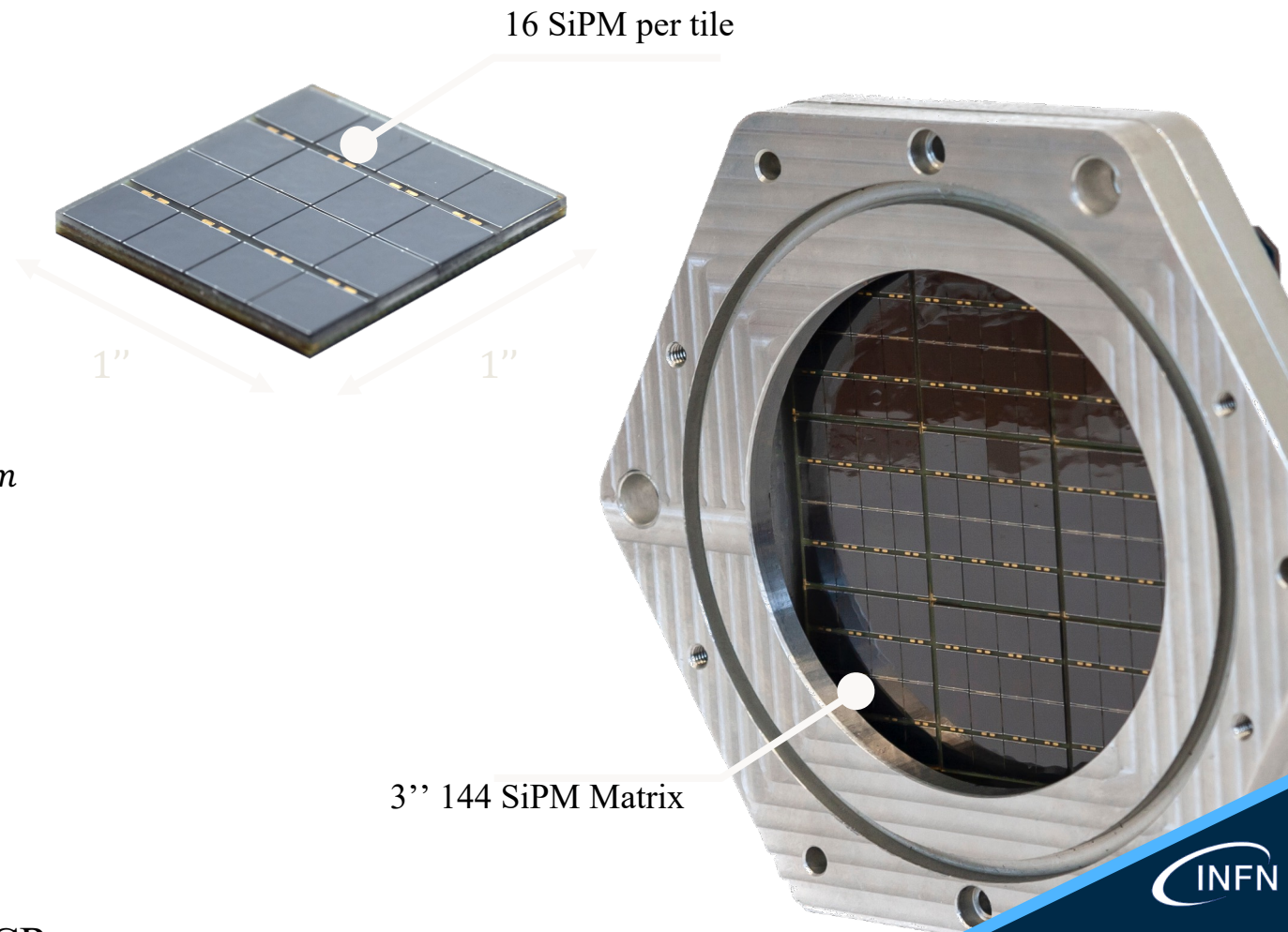
30 μ m cells:

- 45% PDE (photon detector efficiency)
- 77% FF
- $V_{BD} = 26.5V$
- 100kHz/mm² DCR
- 1% non-linearity at **9MeV**

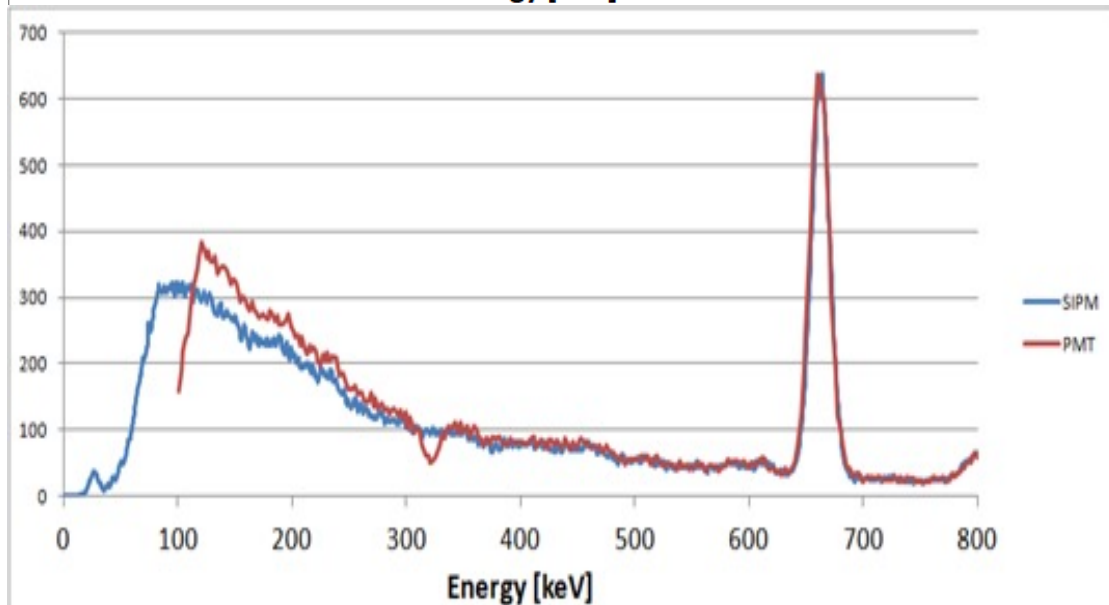
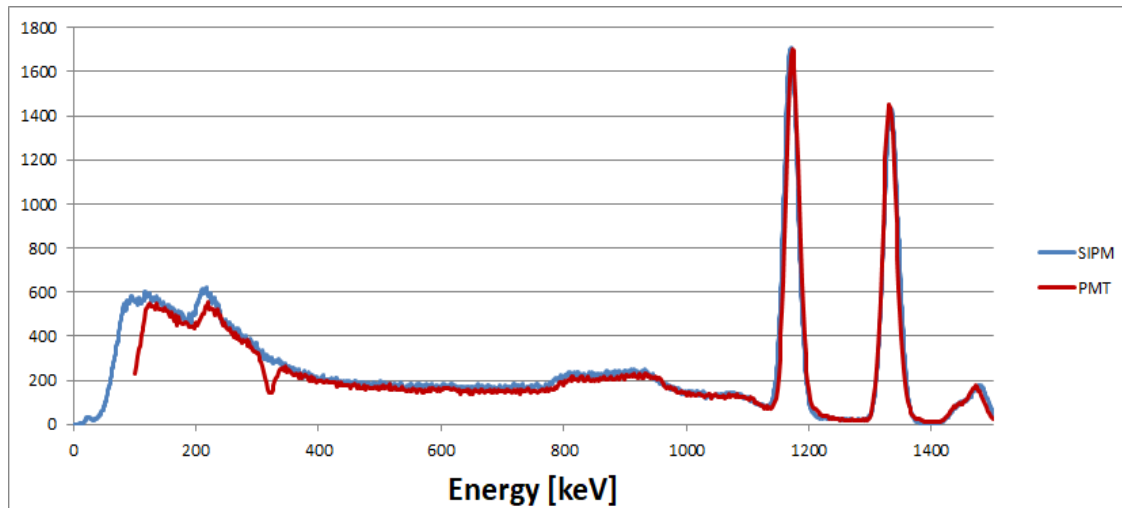


15 μ m cells:

- 35% PDE
- 61% FF
- $V_{BD} = 31.5V$
- 60kHz/mm² DCR
- 1% non-linearity at **35MeV**



LaBr₃:Ce:Sr + SiPMs Comparison with PMT



LaBr₃:Ce:Sr + SiPMs Perspectives

Time performances

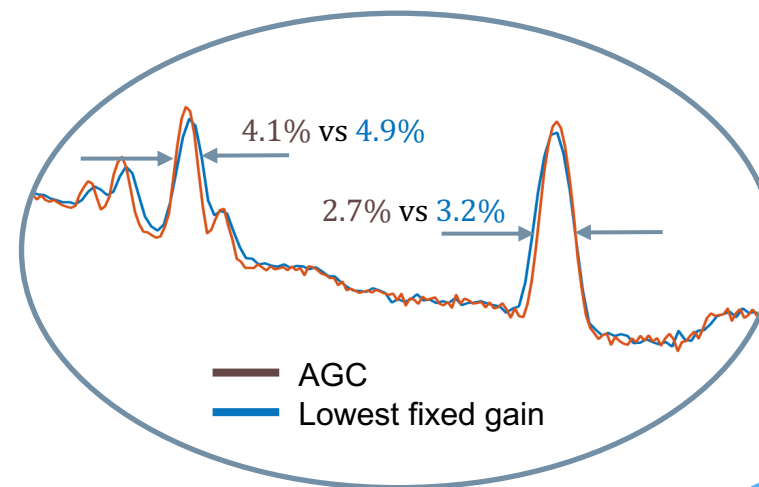
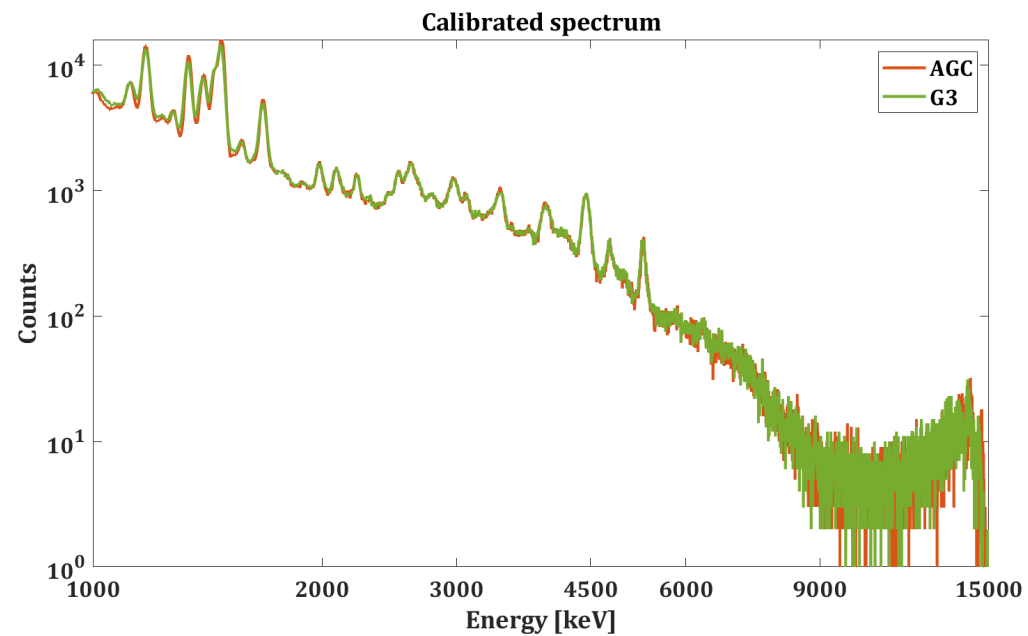
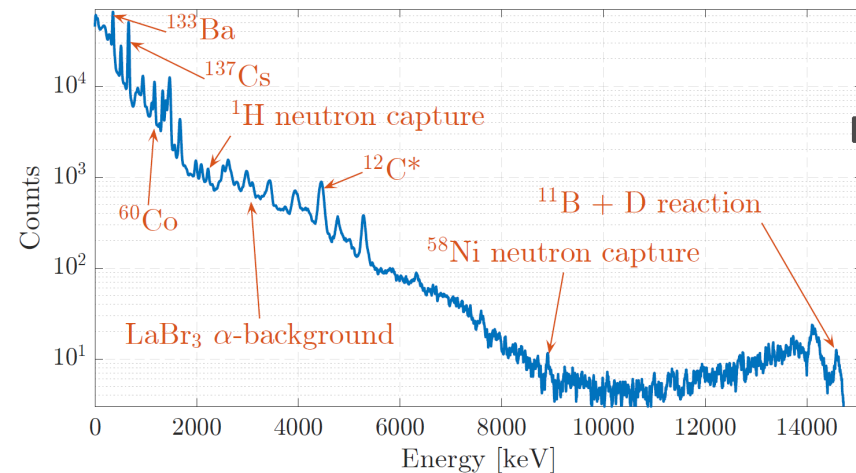
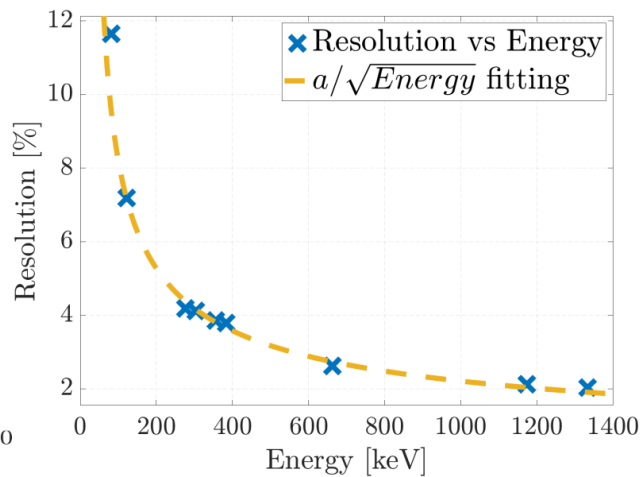
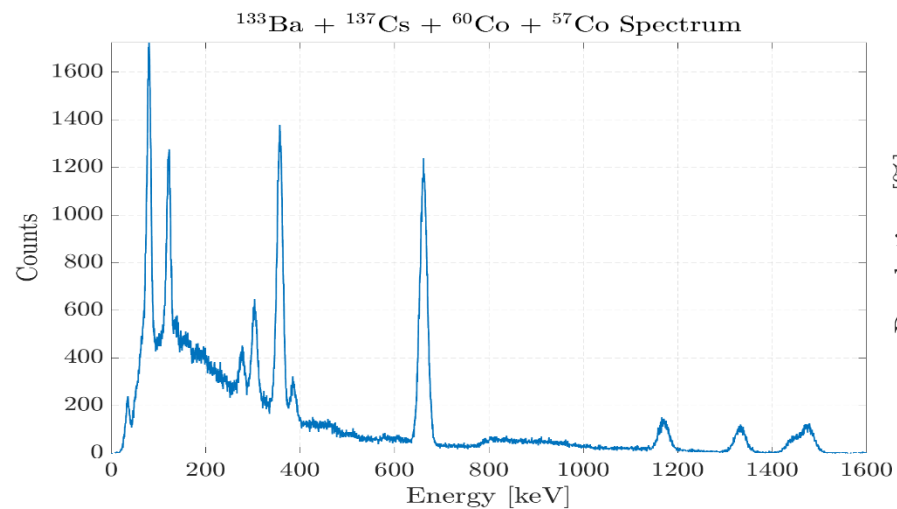
- The used detector has a time resolution of ≈ 2.5 ns
- A new ASIC is going to be developed to improve time performances

Position Sensitivity

- Doppler Broadening reduction

There are no differences between the F.E.P. measured using a PMT and an array of SiPMs

LaBr₃:Ce:Sr + SiPMs



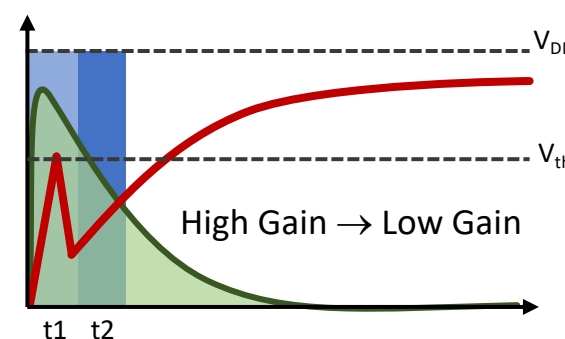
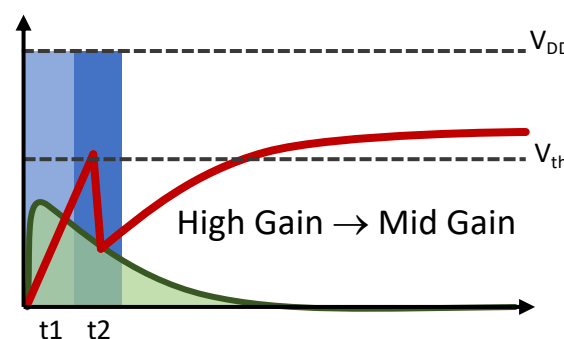
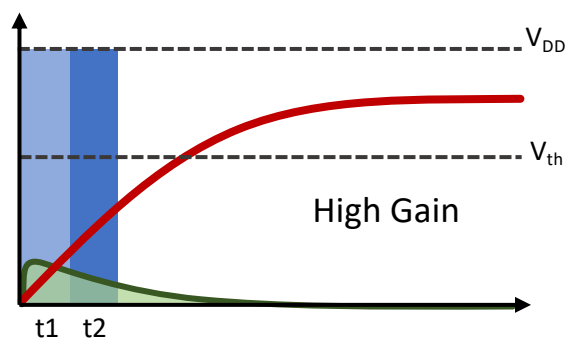
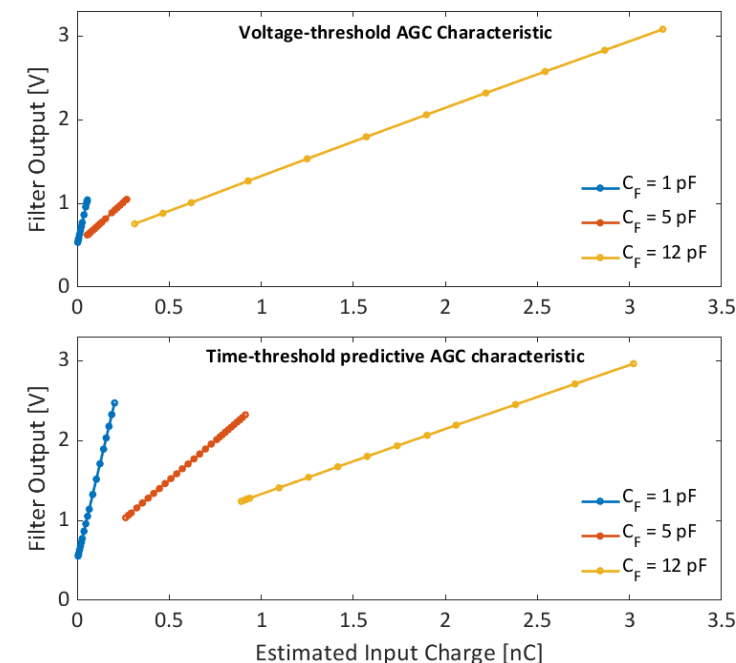
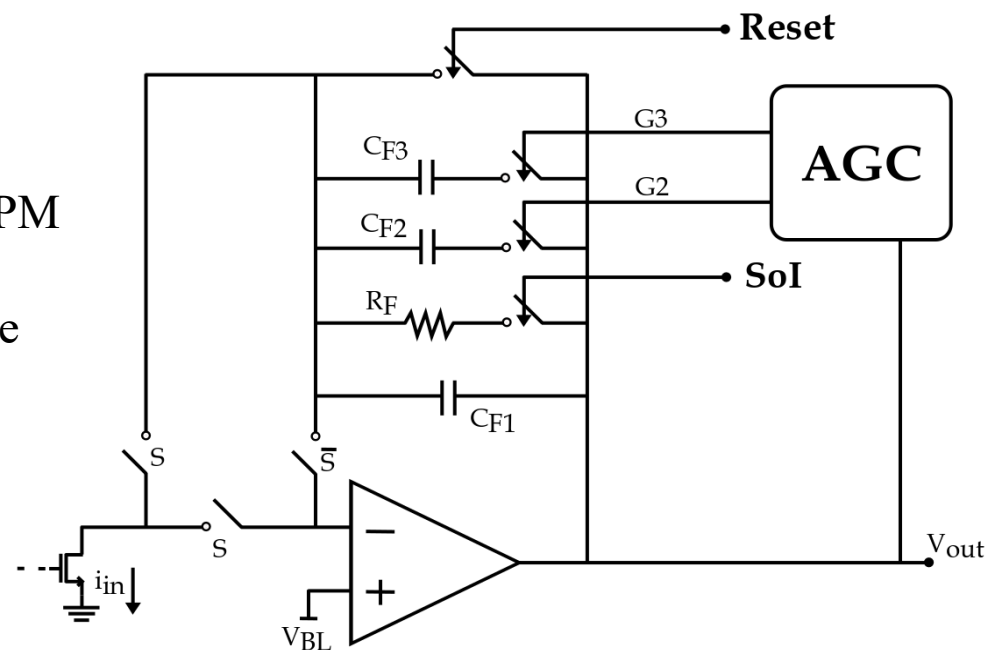
Adaptive gain control (AGV) vs lowest fixed gain



GAMMA ASIC: Adaptive Gain Control (AGC)

GAMMA ASIC:

- 16 channels with AGC
- Stable with $>70\text{nF}/\text{ch}$ (>24 SiPM $6\times 6\text{ mm}^2$ per channel)
- programmable integration time (100ns to $16\mu\text{s}$)
- Monolithic readout

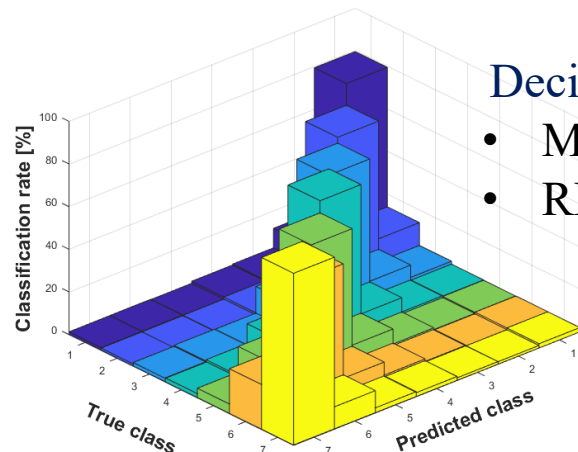


— Input charge
— Output voltage

30keV – 30MeV energy dynamic range in a single measurement

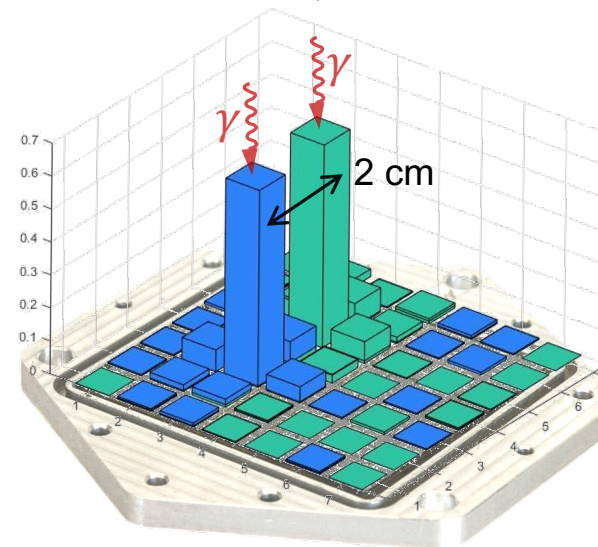
Machine learning for position reconstruction (662 keV)

Confusion matrix (x,y)



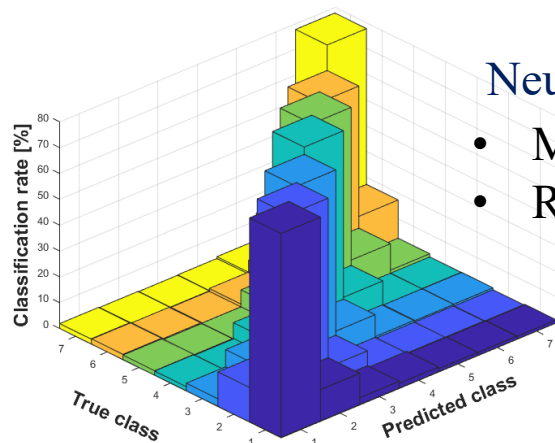
Decision Tree

- Mean error: 0.47 cm
- RMS error: 1.08 cm

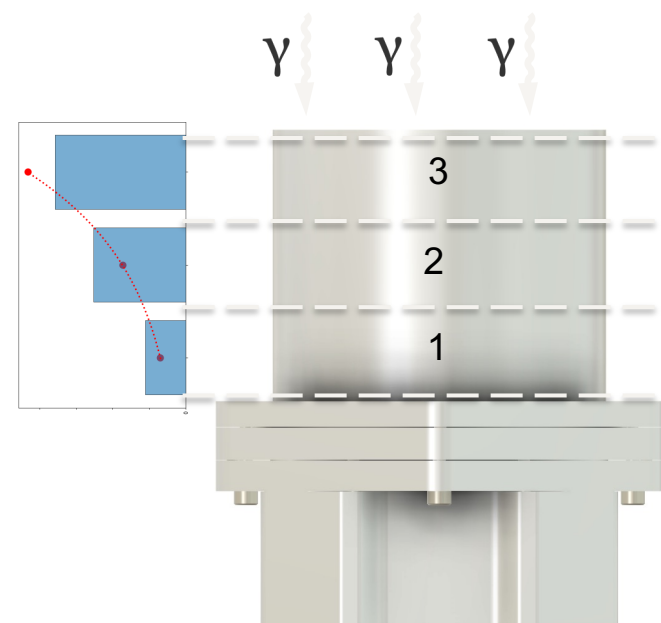


Neural Network

- Mean error: 0.42 cm
- RMS error: 1.02 cm



2 cm spaced irradiations



Depth Of Interaction
(z axis)

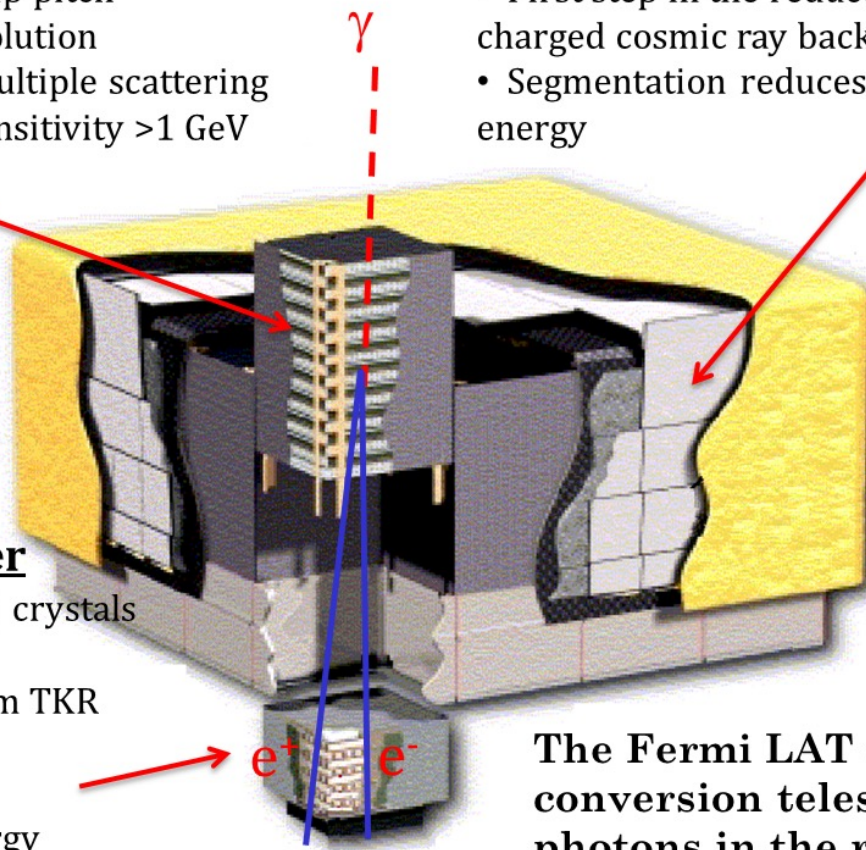
FERMI-GLAST Large Area Telescope

Precision Si-strip Tracker (TKR)

- Measures incident γ -ray direction
- 18 XY tracking planes: 228 μm strip pitch
- High efficiency. Good position resolution
- 12x 0.03 X_0 front end \rightarrow reduce multiple scattering
- 4x 0.18 X_0 back-end \rightarrow increase sensitivity >1 GeV

Anticoincidence Detector (ACD)

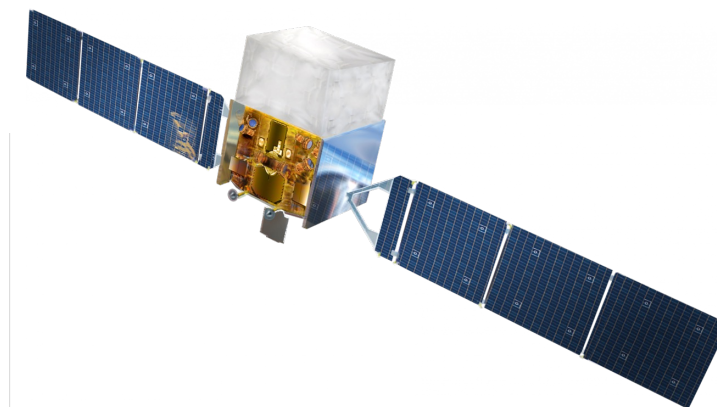
- 89 scintillator tiles
- First step in the reduction of large charged cosmic ray background
- Segmentation reduces self-veto at high energy



Hodoscopic CsI Calorimeter

- Segmented array of 1536 CsI(Tl) crystals
- 8.6 X_0 : shower max contained
 - ~ 200 GeV normal (1.5 X_0 from TKR included)
 - ~ 1TeV @ 40° (CAL-only)
- Measures the incident γ -ray energy
- Rejects cosmic-ray background

The Fermi LAT is a pair-conversion telescope for photons in the range from 20MeV up to >300 GeV



NASA Fermi sat. icon

GLAST Calorimeter

Modular array

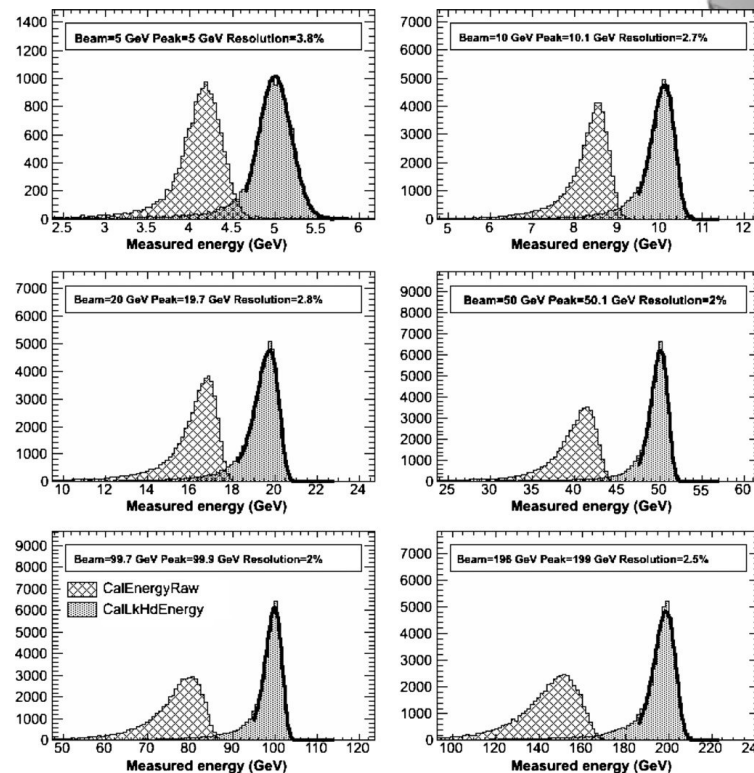
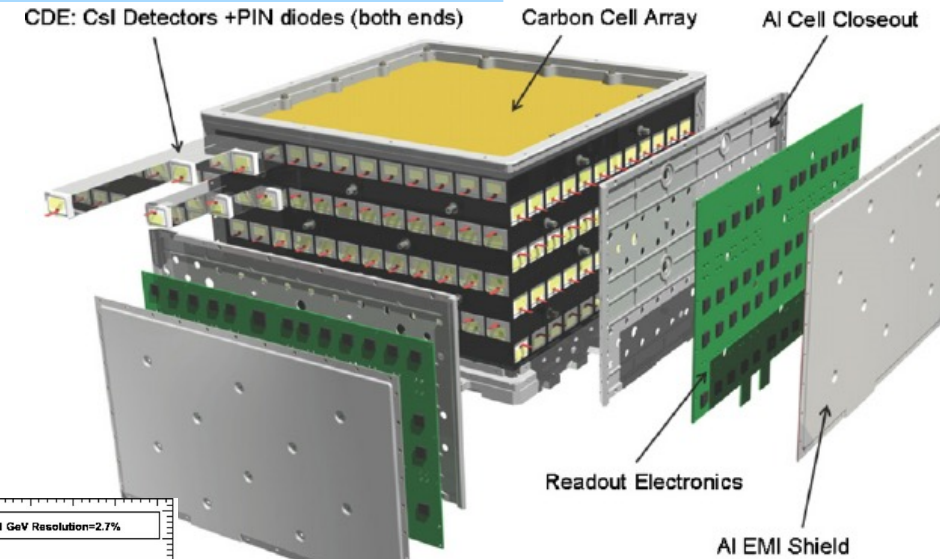
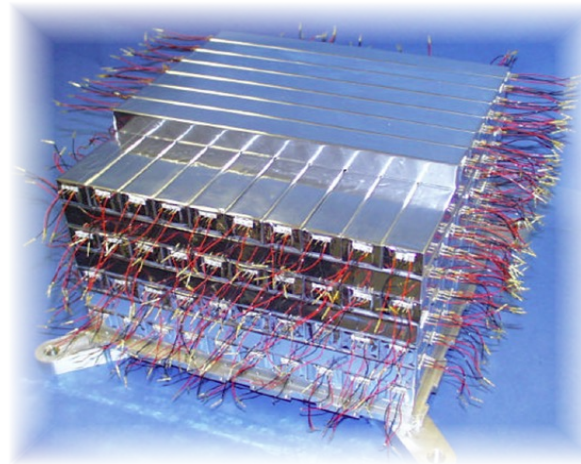
- 4 x 4 CAL modules
- On axis depth = 8.6 R.L.

Each module

- 8 layers of 12 CsI(Tl) crystals
27 x 20 x 326 mm³
- Hodoscopic stacking
Alternating orthogonal layers
- Dual PIN photodiode read-out

Mechanical packaging: Composite cell structure

Electronic boards attached to each side



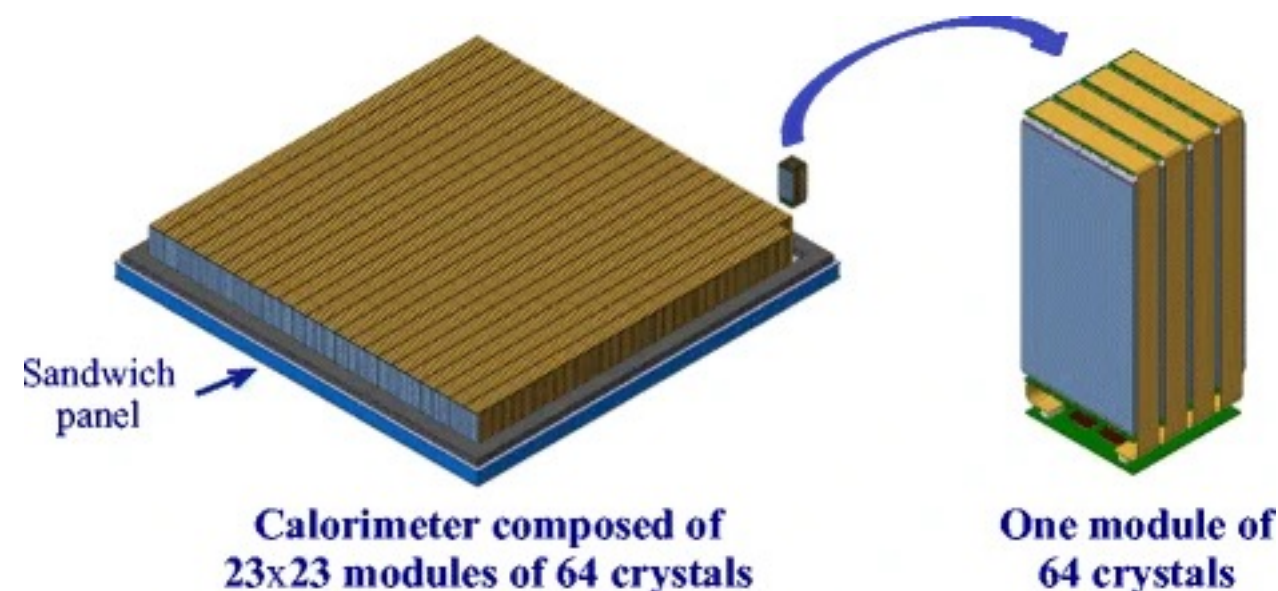
- Energy resolution as a function of electron energy as measured with the LAT calibration unit in CERN beam tests
- Each panel displays a histogram of the total measured energy (hatched peak) and the reconstructed energy (solid peak)
- The beams entered the calibration unit at an angle of 45° to the detector vertical axis

e-ASTROGRAM: calorimeter

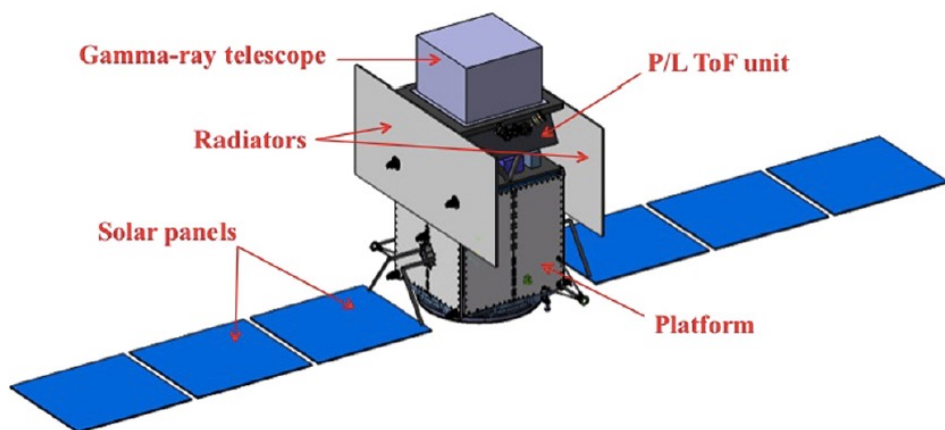
Submitted to ESA M7 call



- ASTROGRAM proposed to ESA M-class call
 - Compton and pair production gamma-ray detector 0.1 MeV \rightarrow 10 GeV.
- CAL module
 - Pixelated detector made of 33856 CsI (Tl) scintillator bars of 8 cm length (4.3 rad lengths) and 5×5 mm² cross section, glued at both ends to low-noise Silicon Drift Detectors (SDDs by FBK) or SiPMs.



e-ASTROGRAM is a proposed space mission with the purpose of measuring gamma rays from astrophysical sources. It will sample the right energies to explore the highest-energy electromagnetic counterparts of gravitational wave events, localizing possible corresponding gamma-ray burst.



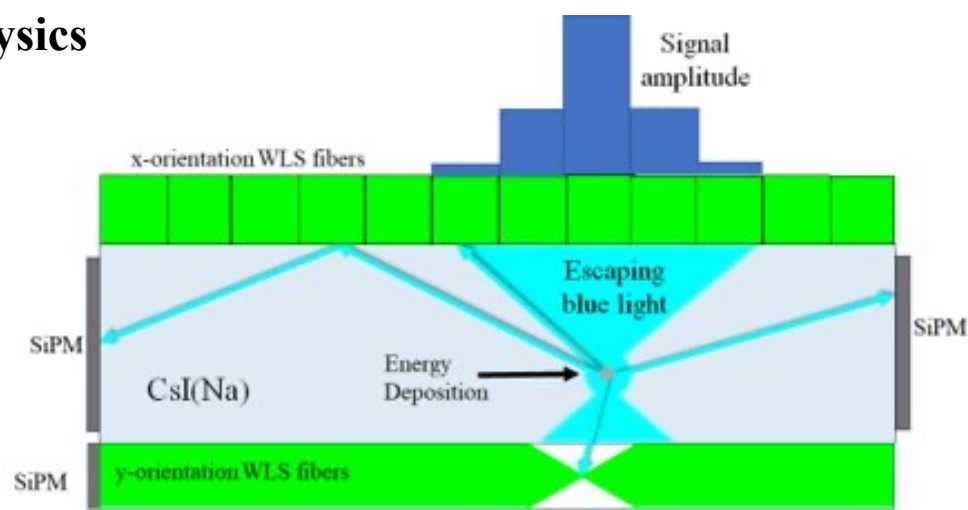
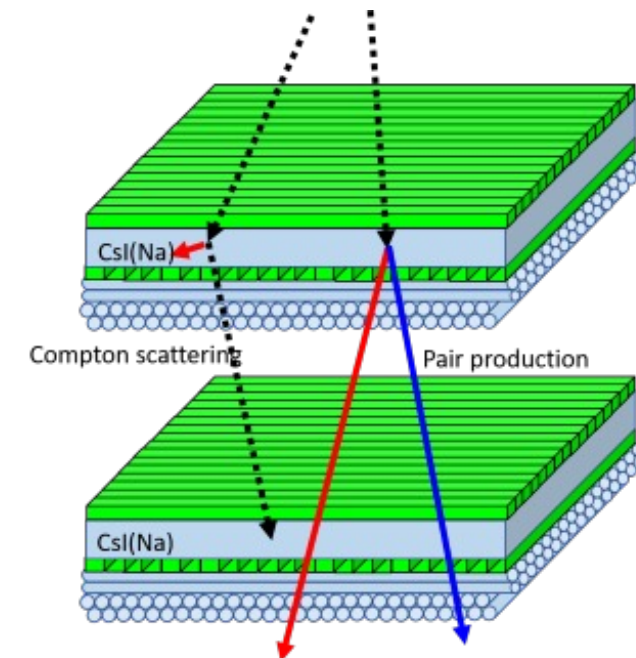
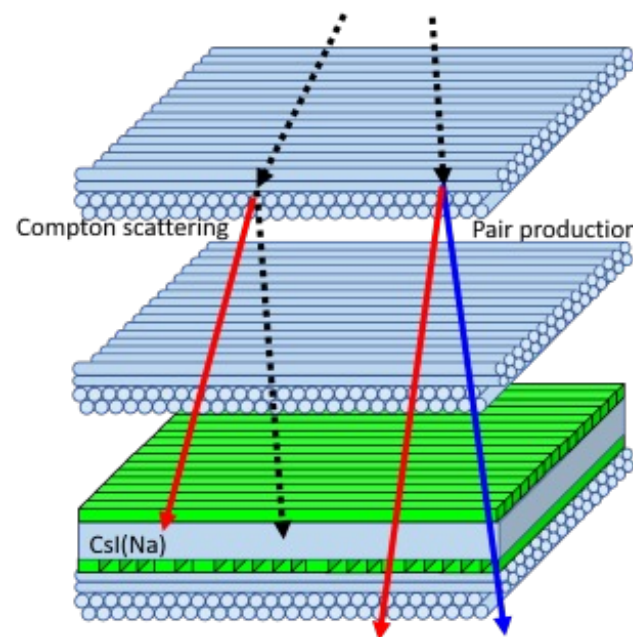
- 1) Astogram coll, *Exp Astron* 44:25–82 (2017)
- 2) A. De Angelis et al. *J. Of High Energy Astrophysics*, 19 (2018)
- 3) Jürgen Knödlseeder, *Comptes Rendus Physique*, 17, 663-678 (2016)
- 4) A. De Angelis et al. arXiv:1611.02232 (2017)

Imaging calorimeter tracker-converter

- Gamma-ray Active tracker-converter based on thin crystal scintillator read-out by external wavelength shifting (WLS) optical fibers

LYSO or CsI(Na) crystals

- Light tracker based on thin plastic scintillating fibers
- Read-out with SiPM linear array at one (or both) end of the fibers
- Based on the **Advanced Particle-astrophysics Telescope (APT)** proposal

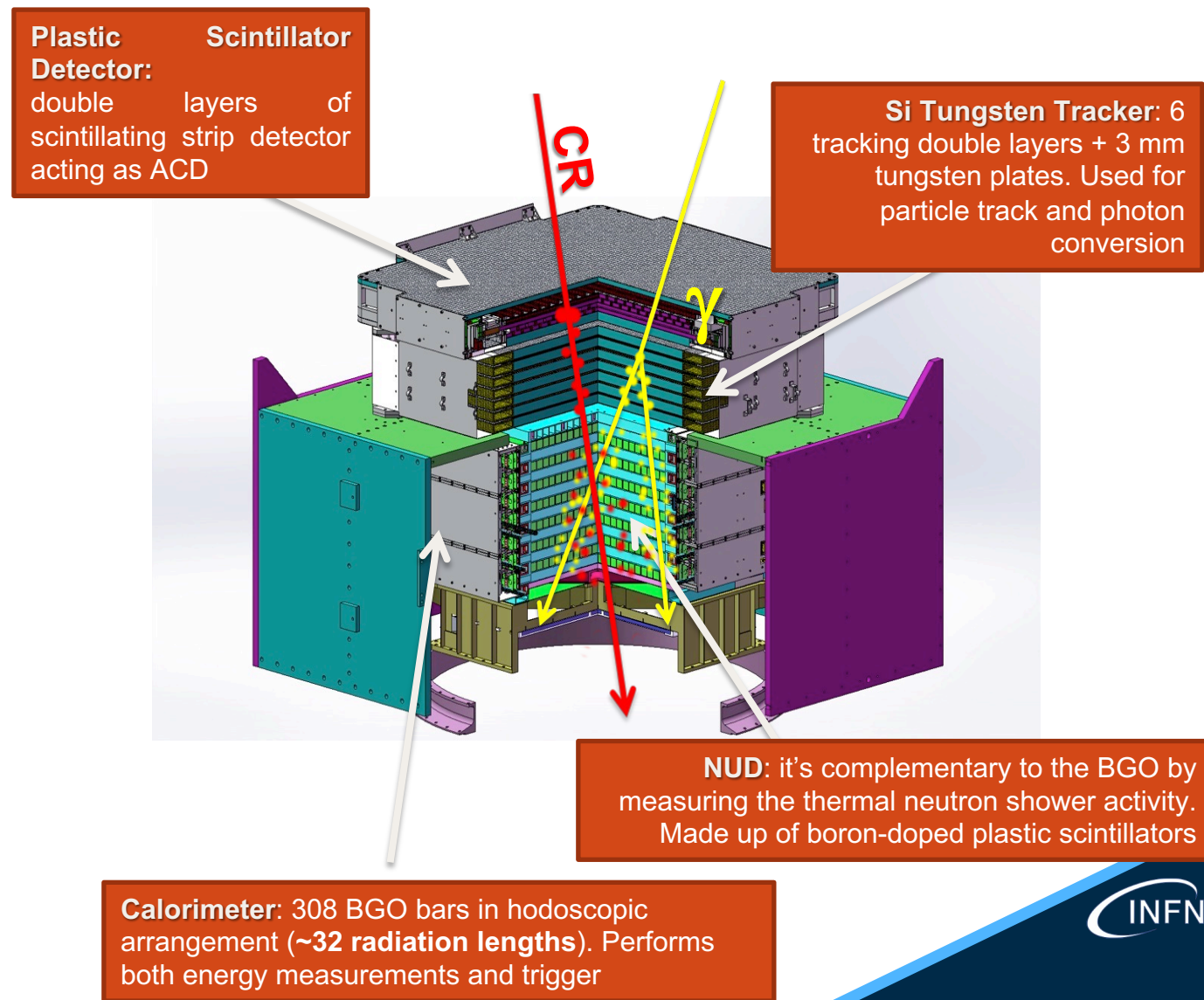


DAMPE project

Dark Matter Particle Explorer dedicated to the indirect detection of dark matter (DM) in space and astrophysical studies.

It was launched to a 500 km Sun-synchronous orbit on Dec. 17th, 2015 from the Jiuquan Satellite Launch Center.

- Si Tungsten Tracker is used as anti-coincidence system for particle bkg rejection for gamma ray detection.
- Photon pair-convert in tungsten plates; energy of positron-electron pairs adsorbed in 14 layer BGO calorimeter (31 rad lengths), read out by PM tubes.



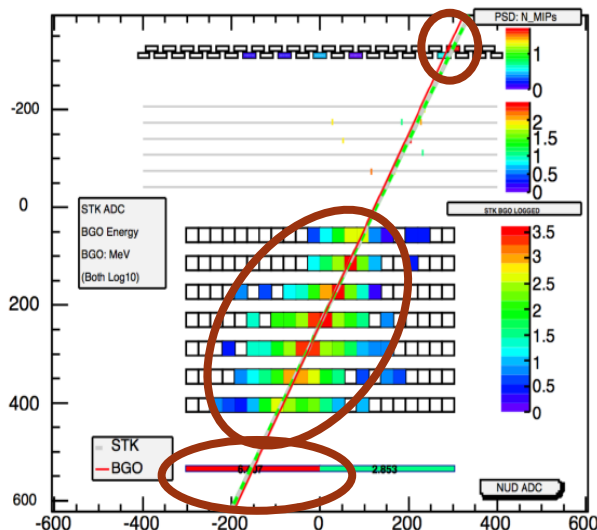
DAMPE: photon selection

The main background sources are proton and electrons:

- Protons: 10^5 @ $E > 100\text{GeV}$ Protons are mainly rejected using the shower profile and the onboard trigger
- Electrons: 10^3 @ $E > 100\text{GeV}$ Electrons are mainly rejected using the PSD and 1st layer of STK

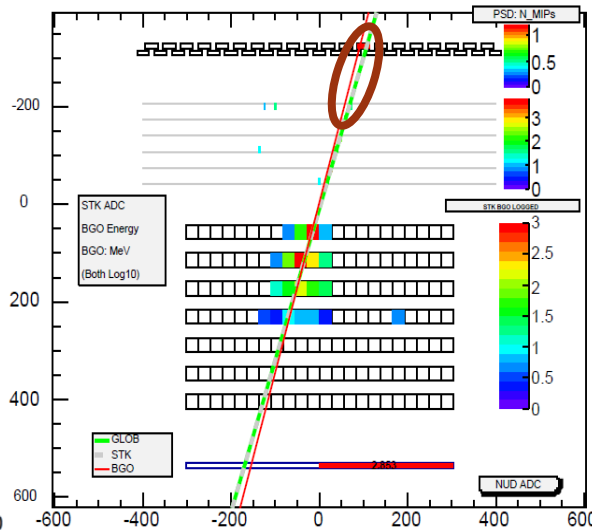
proton

Y [No. 32: 49.132GeV]



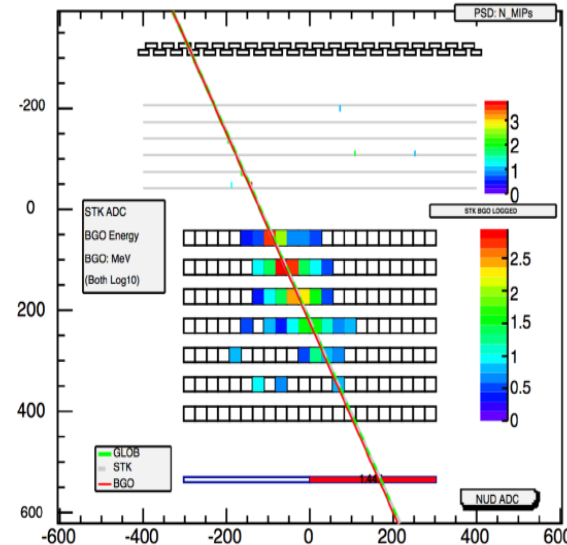
electron

Y [No. 40: 5.034GeV]



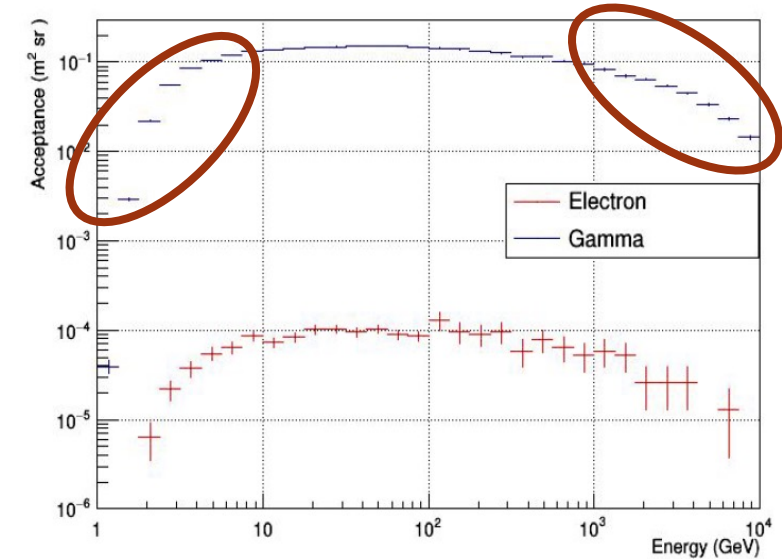
gamma

Y [No. 61: 5.559GeV]



Trigger effect

Backscattering effect

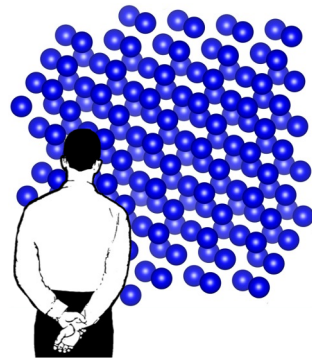


Acceptance after the selection criteria applied to reject protons and electrons.

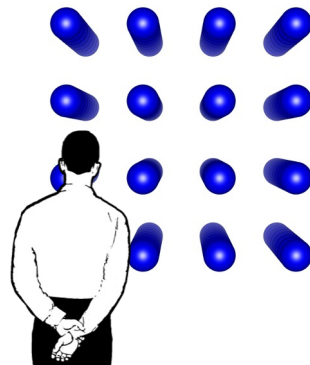
OREO ORiEnted calOrimeter



Randomly Oriented Crystals



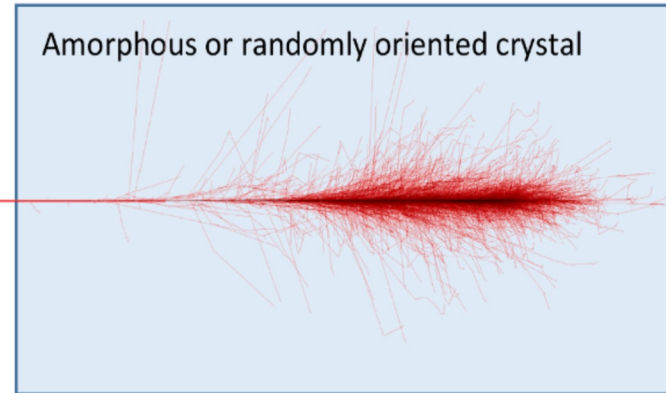
Axially Oriented Crystals



Reduction of the radiation length X_0 in comparison with amorphous media

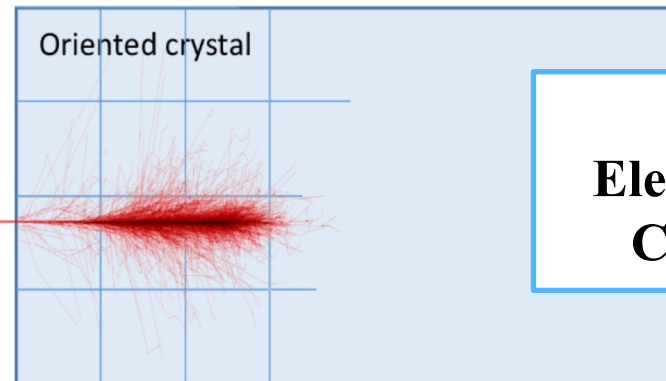
Particle

Amorphous or randomly oriented crystal



Particle

Oriented crystal

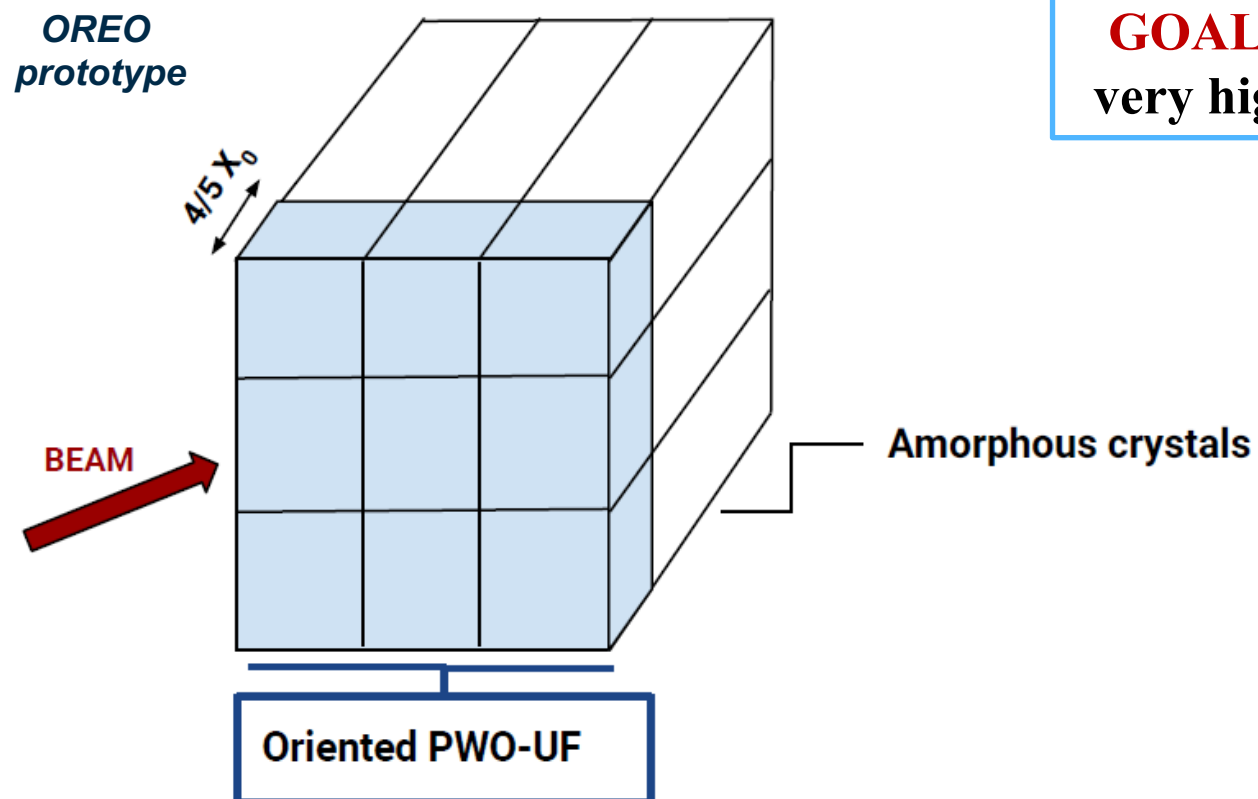


**Compact
Electromagnetic
Calorimeter!**

1) L. Bandiera, *Phys. Rev. Lett* 121 021603 (2018)

For info: bandiera@fe.infn.it

OREO applications



GOAL: to contain electromagnetic showers initiated by very high energy γ/e in a reduced volume/weight and cost

- ❖ *Radiation length reduction*
 - ❖ X_0 decreases with initial energy increase.
- ❖ *Angular range:*
 - ❖ few mrad up to 0.5° - 1° of misalignment between particle direction and crystal axes;
 - ❖ Does **NOT** depend on particle energy.

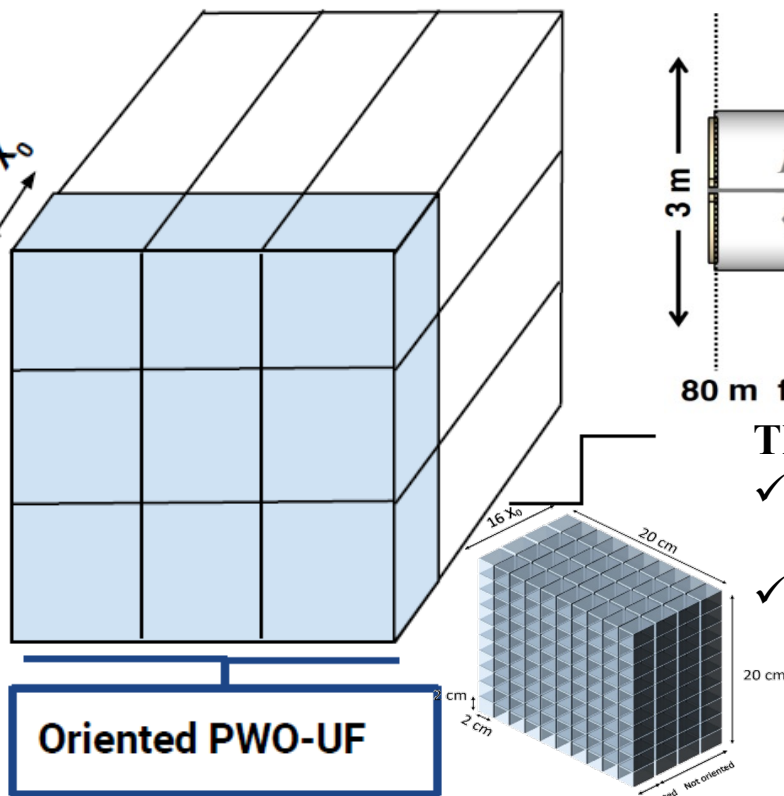
Challenge: Construction of an oriented layer of many crystals

$K_L \rightarrow \pi^0 \nu \bar{\nu}$

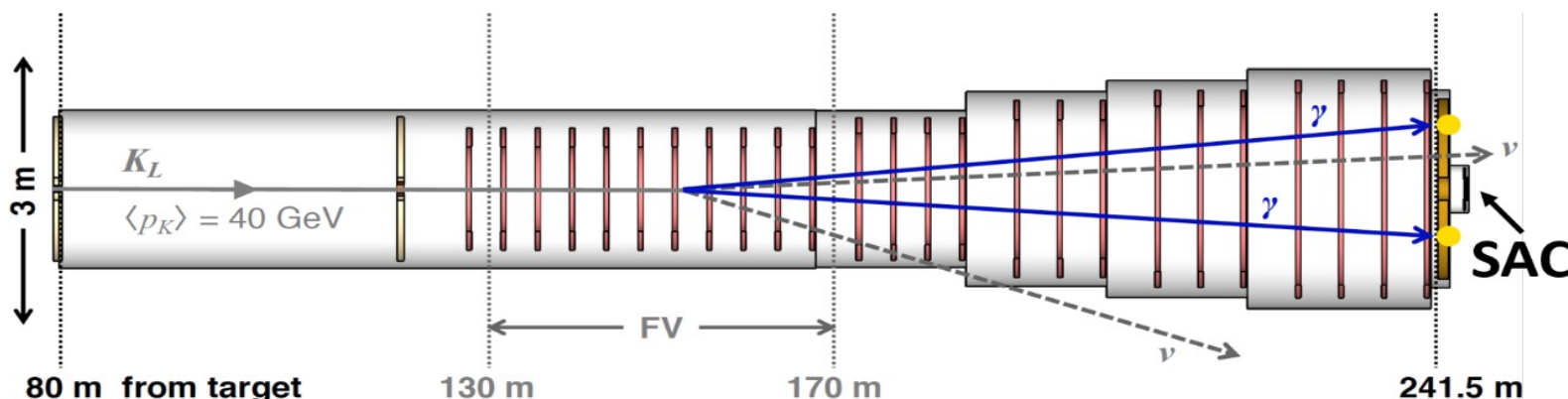
VHE gamma VETO/Small Angle Calorimeter



OREO prototype



KLEVER is a proposed experiment at CERN SPS to measure $K_L \rightarrow \pi^0 \nu \bar{\nu}$



The SAC should:

- ✓ reconstruct the 2 γ of the π^0 coming from $K_L \rightarrow \pi^0 \nu \bar{\nu}$, while any extra photons must be vetoed with very high efficiency!
- ✓ insensitivity to more than 500 MHz of neutral hadrons in the beam.

Challenge:

- Scaling to a large calorimeter
- **The KLEVER SAC ready for 2027!**

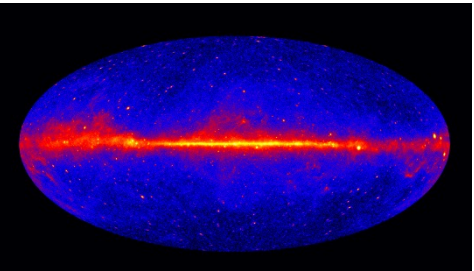
OREO is the best solution for the KLEVER SAC:

- X_0/λ_{int} (radiation length / nuclear interaction length) as smaller as possible, minimizing hadronic interaction and discriminating very well electromagnetic signals.
- Excellent time resolution: Ultrafast PWO

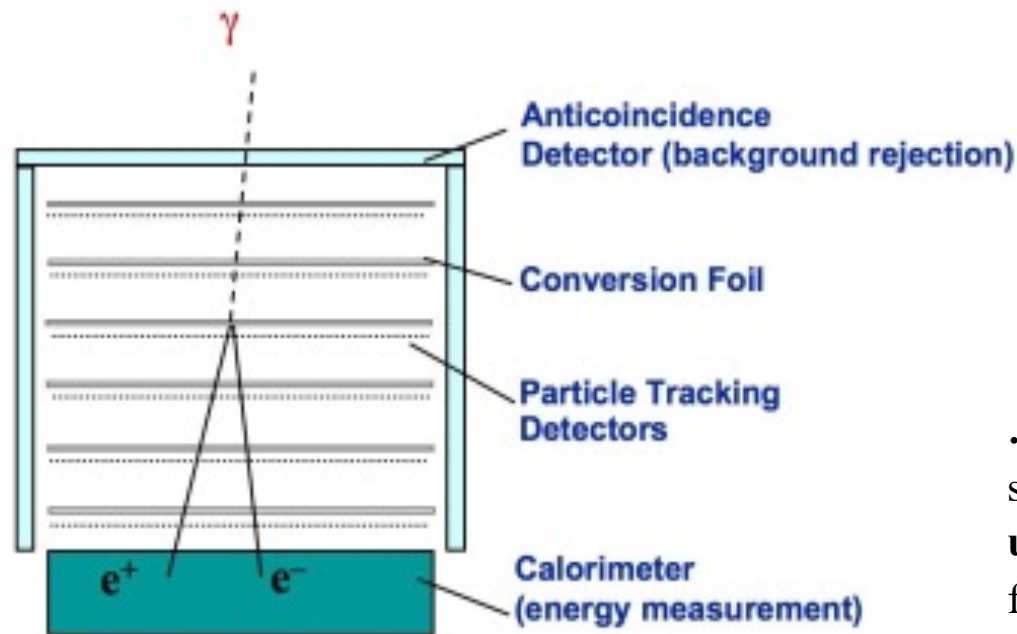
For info: Laura Bandiera and Matthew Moulson



Ultra-compact space-borne gamma-ray telescope based on oriented crystal



Take the FERMI-LAT tower as an example...



All of these materials have a crystalline structure and can be oriented along some preferred lattice direction

If we point a telescope towards a gamma-ray source, we could exploit the X_0 reduction in oriented crystals to...

substitute the W amorphous foils with crystalline W :

- ✓ possible reduction of tracker length and thereby of multiple scattering, with an improvement of the spatial/angular resolution -> better localization of the source;

use oriented scintillator crystals in the calorimeter to:

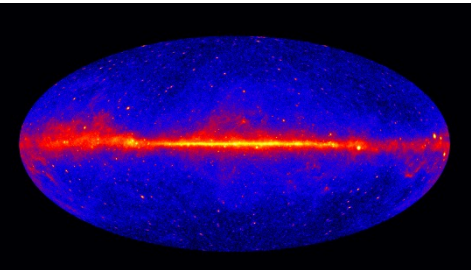
- ✓ enhance the sensitivity of the telescope above few GeV, with a reduced volume/weight -> huge cost reduction!
- ✓ The calorimeter would continue to operate in a standard way in the absence of pointing.

...a variety of possible applications in need of better angular/energy resolution...

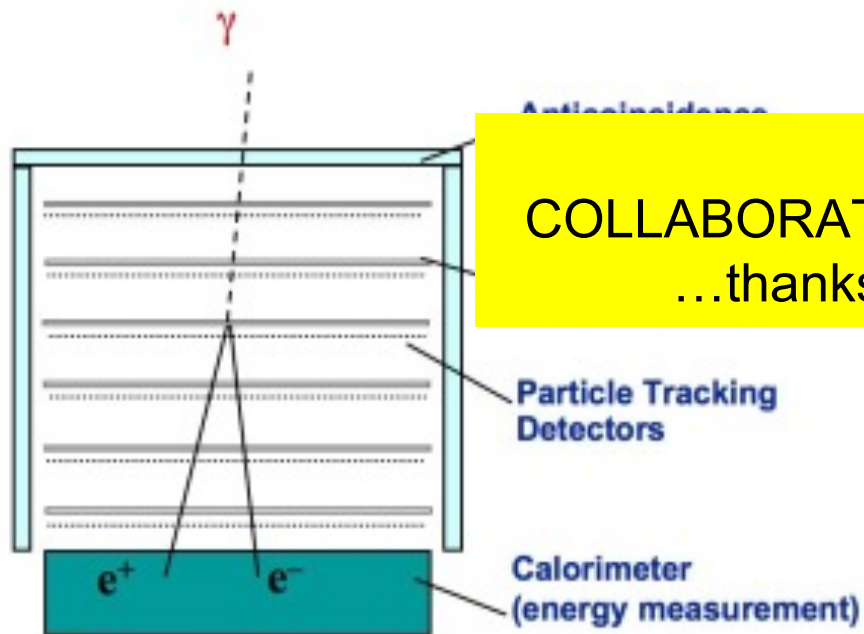
search of **dark matter sources** (galactic centre excess, dwarf galaxies); observation of **unidentified Fermi gamma-ray sources**;

follow-up of flaring/transient and **multi-messenger sources**...

Ultra-compact space-borne gamma-ray telescope based on oriented crystal



Take the FERMI-LAT tower as an example...



All of these materials have a crystalline structure and can be oriented along some preferred lattice direction

If we point a telescope towards a gamma-ray source, we could exploit the X_0 reduction in oriented crystals to...

substitute the W amorphous foils with crystalline W:

- ✓ possible reduction of tracker length and thereby of multiple scattering, with an improvement of the spatial/angular resolution -> better localization of the source;

use oriented scintillator crystals in the calorimeter to:

IDEA AT INITIAL STAGE

COLLABORATION STARTED WITH FERMI-LAT PEOPLE

...thanks to F. Longo, S. Cutini, M. Di Mauro...

, with a reduced volume/weight -

The calorimeter would continue to operate in a standard way in the absence of pointing.

...a variety of possible applications in need of better angular/energy resolution...

search of **dark matter sources** (galactic centre excess, dwarf galaxies); observation of **unidentified Fermi gamma-ray sources**;

follow-up of flaring/transient and **multi-messenger sources**...

For info and new collaborations: Laura Bandiera

Thanks for the attention

- Walter Raniero AGATA array
- Davide De Salvador UNIPD & LNL-INFN
- Stefano Bertoldo LNL-INFN
- Chiara Carraro LNL-INFN
- Stefano Capra MI-INFN
- Alain Goasduff LNL-INFN
- Gilbert Duchene IPHC – Uni. STRASBOURG
- Franco Camera MI-INFN & UNIMI
- Fabio Gargano BA-INFN
- Mario Nicola Mazziotta BA-INFN
- Domenico Santonocito LNS-INFN
- Laura Bandiera FE-INFN



Agenzia Spaziale Italiana



Università
degli Studi
di Ferrara



UNIVERSITÀ
DEGLI STUDI
DI PADOVA